Cement and Concrete Composites 121 (2021) 104088

Contents lists available at ScienceDirect

Cement and Concrete Composites

journal homepage: www.elsevier.com/locate/cemconcomp

Construction and demolition waste-based geopolymers suited for use in 3-dimensional additive manufacturing

Oğuzhan Şahin [a,b], Hüseyin İlcan [a,c], Anıl Tolga Ateşli [c], Anıl Kul [a,c], Gürkan Yıldırım [c], Mustafa Şahmaran [c,*]

[a] Hacettepe University, Institute of Science, Beytepe, Ankara, Turkey
[b] Department of Civil Engineering, Kırşehir Ahi Evran University, Kırşehir, Turkey
[c] Department of Civil Engineering, Hacettepe University, Ankara, Turkey

ARTICLE INFO

Keywords:
Geopolymer
Construction and demolition waste (CDW)
3-Dimensional additive manufacturing (3D-AM)
Rheology
Alkaline activator

ABSTRACT

This paper focuses on the evaluation of ambient-cured 100% construction and demolition waste (CDW)-based geopolymers in terms of rheological properties for 3-dimensional additive manufacturing (3D-AM). The CDW-based precursors used for geopolymer production were hollow brick (HB), red clay brick (RCB), roof tile (RT) and glass (G) activated by different combinations of sodium hydroxide (NaOH), calcium hydroxide ($Ca(OH)_2$) and sodium silicate (Na_2SiO_3). Rheological properties were evaluated via empirical tests such as flow table, vane shear test, modified mini-slump test and compressive strength test for mechanical characterization. Based on these results, the extrudability performance of selected CDW-based geopolymer mixtures was analyzed with a ram extruder, and finally, a single mixture was selected to be used in laboratory-scale 3D-printing. The geopolymer mixture activated by 6.25 M NaOH and 10%-$Ca(OH)_2$ exhibited the best performance in terms of rheology and compressive strength, and it was therefore selected for use in laboratory-scale 3D-printing. 3D-AM application at the laboratory scale showed that ambient-cured 100% CDW-based geopolymers can be successfully used for 3D-printing, with adequate rheological and mechanical properties and without any additional chemical admixtures, and that the empirical test methods used are effective in assessing the suitability of CDW-based geopolymers for 3D-AM applications. The outcomes of this work are believed to contribute to the current literature significantly, as they combine the advantages of green material development, waste upcycling, reduced raw materials and easy/fast/accurate producibility.

1. Introduction

Despite being the most widely used construction material, concrete brings about considerable challenges. Portland cement (PC), which is the main binding material for traditional concrete, has enormous negative environmental impacts, mainly due to the high energy requirement for its production and the associated release of greenhouse gases [1]. Production of PC and concrete require the use of natural resources such as clean water, different-size aggregates, clay, limestone and gypsum, leading to addition effects that are detrimental to the environment [2]. Minimizing the use of cementitious materials can help reduce energy consumption, CO_2 emissions and raw material use, which makes it an important step in reaching global environmental sustainability goals. Researchers have therefore been working to develop environmentally-friendly construction materials capable of minimizing energy and natural resource consumption [3,4]. These efforts have resulted in a novel generation of binder materials called alkali-activated materials or geopolymers, which are successful candidates as partial or full substitutes for PC.

Geopolymers are inorganic polymers formed as a result of the reaction between aluminosilicate source materials (i.e. precursors) and alkaline activators (e.g. solutions of alkali-hydroxide/-silicate) [5]. Among different aluminosilicate precursors used in geopolymer technology, mineral admixtures such as blast furnace slag, fly ash, silica fume and metakaolin are prevalent, while sodium hydroxide potassium hydroxide, calcium hydroxide, sodium silicate are more commonly used as alkaline activators [6]. Although geopolymers can be successfully produced by the aluminosilicate precursors listed above, these precursors are in high demand, given their successful use in blended PC and concrete mixtures as mineral admixtures. Moreover, these mineral

* Corresponding author.
E-mail address: sahmaran@hacettepe.edu.tr (M. Şahmaran).

https://doi.org/10.1016/j.cemconcomp.2021.104088
Received 11 February 2021; Received in revised form 29 April 2021; Accepted 2 May 2021
Available online 12 May 2021

admixtures, which were formerly considered troublesome, are sometimes sold at prices comparable to or even higher than that of PC, taking into account their well-established benefits to PC and concrete. Therefore, increasing attention is now being paid to aluminosilicate precursors not as highly demanded by the cement and concrete industry [7].

As cities transform, millions of buildings that are at the end of their service lives (or in a state that is dangerous to their occupants and the environment) are being demolished. So what can be done with the huge amounts of resulting construction and demolition waste (CDW)? This is the question that is under debate globally. CDW mostly ends up being stored and landfilled, which requires immense space and is very costly in terms of health, economy and environment [8]. The capabilities of most countries to properly handle CDW vary significantly, and are mostly limited to old-fashioned methods such as direct crushing and road base/sub-base filling. That necessitates the development of innovative and effective ways to deal with CDW, especially for developing and economically struggling countries. One effective way to handle CDW disposal is to use CDW-based components to produce geopolymers. CDW generation is a global issue and can be easily found almost anywhere in the world [9,10].

Studies focusing on the development of geopolymers using CDW-based precursors (e.g. concrete, bricks, tiles, ceramics, glass) are available in literature, although they are significantly less common than studies using mainstream aluminosilicates. In one such study, Allahverdi and Kani [11] performed experiments on the alkali-activation of waste concrete and bricks. They found that paste produced from brick wastes and subjected to certain curing conditions reached 28-day compressive strength of up to 40 MPa, while using concrete waste for alkali-activation was not as effective. Reig et al. [12] manufactured geopolymer mortars from CDW-based ceramic waste and concluded that depending on the sodium concentration of the alkaline activator and water-to-binder ratio, compressive strength between 22 and 41 MPa can be obtained for mortars cured at 65 °C for 7 days. Komnitsas et al. [13] produced geopolymers using CDW-based concrete, tile and brick activated by sodium hydroxide and sodium silicate solutions. Compressive strength tests were performed on geopolymers manufactured with varying activator ratios and subjected to different curing conditions. Concrete-, brick- and tile-based geopolymers reached 7-day compressive strength results of 13.0, 49.5 and 57.8 MPa, respectively. Silva et al. [14] used fire clay brick as a precursor in producing geopolymers by proposing different conditions for geopolymerization. Their results revealed that with proper conditioning (i.e. silica modulus of 0.60, Na_2O content of 8%, water-to-binder ratio of 0.27 with 7-day oven curing between 65 and 80 °C), a compressive strength level of 37 MPa could be reached. Robayo-Salazar et al. [15] used red clay brick, concrete and glass originating from CDW, singly or as replacement for PC, as precursors in developing alkali-activated building materials. The study concluded that although using CDW-based components was successful in achieving acceptable mechanical properties, results were better in the case of CDW and PC blends. Glass waste, one of the most common CDW constituents, has also been used as precursor, activator and aggregate to develop geopolymer systems, as reported by Ulugöl et al. [9], Xiao et al. [16], Torres-Carrasco and Puertas [17], Cyr et al. [18], and Vafaei and Allahverdi [19]. A recent paper extensively discussed geopolymer systems developed using CDW-based constituents as precursors singly or in combination with traditional mineral admixtures [20]. As clearly shown by these literature studies, CDW-based precursors can be successfully used in geopolymer production. However, the subject requires further attention to adequately advance our knowledge of CDW-based geopolymer systems, which is significantly lacking compared to geopolymer systems based on mainstream precursors.

In addition to the emphasis placed on developing a new generation of environmentally-friendly construction materials, using advanced manufacturing technologies in the production processes of such materials has also been a recent focus. One of these production technologies that is quite popular is additive manufacturing (AM), which can basically be defined as layer-by-layer production. With the development of technology, the AM of concrete structures has been adopted as an approach that overcomes several difficulties faced by the existing concrete industry. For example, three-dimensional (3D) AM technology enables non-molded construction with greater speed and minimum human error [21]. Avoiding molding in construction reduces the total cost by 30–60%, as molding is one of the most costly facets of construction [22]. 3D-AM technology also offers much more design freedom and flexibility than traditional construction methods. Additionally, it has real advantages in terms of occupational safety, since it is remote-controlled and does not require additional workers during on-site implementation [23].

Several recent studies have explored combining the notable advantages of geopolymers from an innovative materials perspective and 3D-AM technology from an advanced materials processing perspective. Panda et al. [24] analyzed factors affecting the tensile bond strength of geopolymers with a precursor of combined fly ash, ground granulated blast furnace slag and silica fume, activated by potassium silicate solution. The factors were the fresh and hardened properties of the casted material, the time difference between layer castings, nozzle speed and nozzle-to-datum height (or casting surface). Another study was performed on the flexural characteristics of geopolymers produced by 3D-AM technology and reinforced by hybrid polyvinyl alcohol fiber and steel wire [25]. Geopolymers were based on fly ash, ground granulated blast furnace slag and silica fume as the precursor combination, and potassium silicate as the alkaline activator. Results showed that compared to control sample, using a hybrid fiber reinforcement was capable of increasing the flexural performance of geopolymers by up to 290%. Panda and Tan [26] studied the rheological properties of geopolymer mortars with fly ash, ground granulated blast furnace slag and silica fume, and activated by a combination of potassium silicate and sodium hydroxide. They evaluated the extrudability, shape retention, thixotropy and buildability characteristics of geopolymer mortars. The rest of the studies also focused on the production of geopolymers based on 3D-AM technology [27–31] using mainstream precursors, most probably due to the controlled and well-known properties of these materials. However, no studies have been encountered in the literature regarding the development of CDW-based geopolymers via 3D-AM technology.

In this study, geopolymers were produced by using CDW-based components via 3D-AM technology, with a primary focus on fresh/rheological properties due to their importance for proper producibility in digital fabrication. This work is novel in that using CDW-based components to manufacture geopolymers via 3D-AM technology combines the advantages of green material development, waste upcycling, reduced need for raw materials and easy/fast producibility. CDW-based components used as precursors were clay-originated masonry units including hollow brick (HB), red clay brick (RCB) and roof tile (RT) along with waste glass (G). HB, RCB and RT were used in combination with G to balance the Si/Al ratio of the mixtures. CDW-based masonry units and glass were chosen over other CDW components based on the fact that masonry constitutes large proportion of CDW and the recycling rate of glass is low.

Sodium hydroxide (NaOH), sodium silicate (Na_2SiO_3) and calcium hydroxide ($Ca(OH)_2$) were used as different alkaline activators and their single, binary and ternary combination effects on the rheological properties of CDW-based geopolymers were determined. Simple empirical test methods such as flow table, vane shear test, modified mini-slump test (for buildability) were used to determine the most suitable rheological/workability parameters for the optimized performance of 3D printable 100% CDW-based geopolymer composites. The 3D-printing process was simulated via a ram extruder to determine the rheological parameters and extrusion force required for proper printing operation without defect or discontinuity. Finally, the printability of the ultimate 100% CDW-based mixture was validated via a laboratory-scale 3D-

printer.

2. Experimental program

2.1. Materials

CDW-based precursors used in producing geopolymers were hollow brick (HB), red clay brick (RCB), roof tile (RT) and glass (G). Assorted CDW components were obtained from demolitions in Eskisehir, Turkey. After being acquired, they were loaded individually into a jaw crusher, which applied primary crushing to reduce precursor size. Initial crushing was followed by a final milling in a ball mill for 1 h. After milling process, oxide compositions (Table 1) and particle size distributions (Fig. 1) of the precursors were determined by using X-ray fluorescence (XRF) analysis and laser diffraction method, respectively. During XRF analysis, wavelength of 0.1–50 Å was used while during the laser diffraction method, a particle size range sensivity of 0.02–2000 μm was used. Moreover, specific gravity and physical appearance of milled CDW-based precursors were given in Table 1 and Fig. 2, respectively. Fig. 3 shows the images of the precursors obtained by using a scanning electron microscope (SEM), operated at 12 kV under vacuum condition with a working distance of 10 mm. The major oxides for the clay-originated CDW components (HB, RCB, RT) were SiO_2 and Al_2O_3, followed by Fe_2O_3, which are the main oxides needed for geopolymerization reactions. Proportions of the major oxides for these precursors were similar, while the oxide composition of G was different than the rest of CDW-based precurors. G, obtained from window glasses, was soda-lime-based and had high SiO_2 (66.5%) followed by NaO (13.6) and CaO (10.0) contents.

After constant milling for 60 min, the CDW-based precursors reached different grain size distributions. As seen from Fig. 1, RT and RCB had similar granulometries and were slightly finer than HB, while G was the coarsest. About 95% of the grains of RT, RCB and HB were finer than 45 μm. However, G remained coarser, with about 70% of its grains finer than 45 μm. Before final milling, it was presumed that different CDW-based precursors would have different grain sizes, given their different hardnesses. However, no special attention was paid to make the precursors finer and the constant grinding period of 1 h was not extended. Instead, the study considered the future possibility of milling relatively different types of CDW-based precursors together to better simulate actual field conditions, where different types of CDW are obtained collectively rather than in an assorted way. Moreover, to make CDWs (specifically glass) smaller in grain size requires additional steel balls with different dimensions and longer milling periods that can be less energy-efficient and more costly and time-consuming. The grinding process caused all the CDW-based precursors to have an angular shape, as seen from the SEM micrographs, showing the morphology of the precursors.

Table 1
Oxide compositions and specific gravity of CDW-based precursors.

Oxides, %	Hollow brick (HB)	Red clay brick (RCB)	Roof tile (RT)	Glass (G)
SiO_2	39.7	41.7	42.6	66.5
Al_2O_3	13.8	17.3	15.0	0.9
Fe_2O_3	11.8	11.3	11.6	0.3
CaO	11.6	7.7	10.7	10.0
MgO	6.5	6.5	6.3	3.9
Na_2O	1.5	1.2	1.6	13.6
K_2O	1.6	2.7	1.6	0.2
SO_3	3.4	1.4	0.7	0.2
TiO_2	1.7	1.6	1.8	0.1
P_2O_5	0.3	0.3	0.3	–
Cr_2O_3	0.1	0.1	0.1	–
Mn_2O_3	0.2	0.2	0.2	–
Loss on ignition	7.8	8.0	7.5	4.3
Specific gravity	2.9	2.8	2.9	2.5

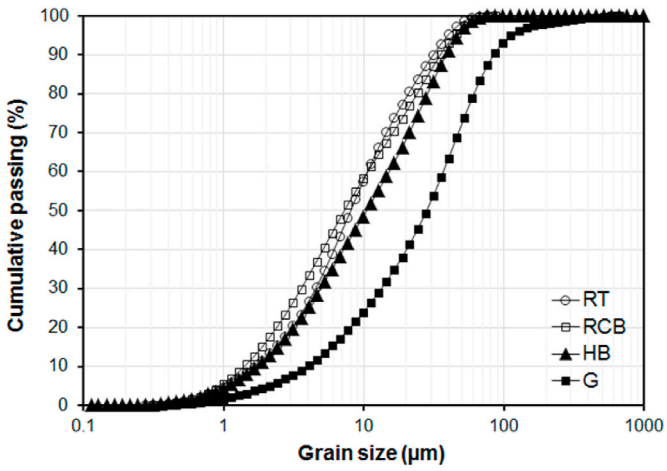

Fig. 1. Grain size distributions of CDW-based precursors.

Crystalline phases of the CDW-based precursors were determined by X-ray diffraction (XRD) analysis and shown in Fig. 4. The analysis was performed by using Olympus BTX Benchtop XRD Analyzer and scanning the dry samples between 5 and 55° with an increment of 0.02°. XRD patterns of the clay-originated precursors had amorphous to semi-crystalline phases and were similar to each other, with a broad hump centered mainly around 2θ of 27–29° and varying crystalline peaks of different intensities. As expected, the quartz phase was the major crystalline peak, with the highest intensity for RCB, RT, and HB. The other major peaks were diopside for all masonry units. Crystalline phases detected for different CDW-based precursors are shown in Table 2. G was of an amorphous nature, with a broad peak centered at approximately 2θ values of 28°.

For the alkaline activation of CDW-based precursors, sodium hydroxide (NaOH), sodium silicate (Na_2SiO_3) and calcium hydroxide ($Ca(OH)_2$) were used in different combinations. Details of the alkaline activator selection are discussed in the section devoted to mixture proportions. NaOH was in flake form and its composition was a minimum 98% sodium hydroxide, maximum 0.4% sodium carbonate, 0.1% sodium chloride and a maximum 15 ppm iron. Na_2SiO_3 was in a liquid state, with water content of 45% and silicate modulus (SiO_2/Na_2O) of 1.9. $CaOH_2$ was in powder form with a purity of 87%.

2.2. Mixture proportions

As noted previously, the SiO_2 and Al_2O_3 contents of clay-originated precursors were similar in terms of grain size distribution. In this regard, a base mixture was produced as a reference to further modify the rheological properties/compressive strength of the mixtures via changes in precursor composition and alkaline-activator type/concentration. Given the similarities in the physical and chemical properties of RCB, RT and HB, the base mixture incorporated equal amounts of clay-originated precursors. By doing so, the combined use of CDW-based precursors was assured, which is more representative of actual field conditions where CDW is obtained collectively. In an effort to improve the collective use of CDWs, the blend of clay-originated CDWs used in the base mixture was substituted with the G precursor by 10% of the total weight of precursors. This was done to back the overall SiO_2 content of the collective base mixture, and to complement the significantly low Al_2O_3 content in the G precursor. The substitution rate of G precursor was selected in order to not disturb the Si/Al balance of the mixtures, which can lead to the formation of a weak microstructure and lower mechanical performance [32].

Different types and combinations of alkaline activators were used

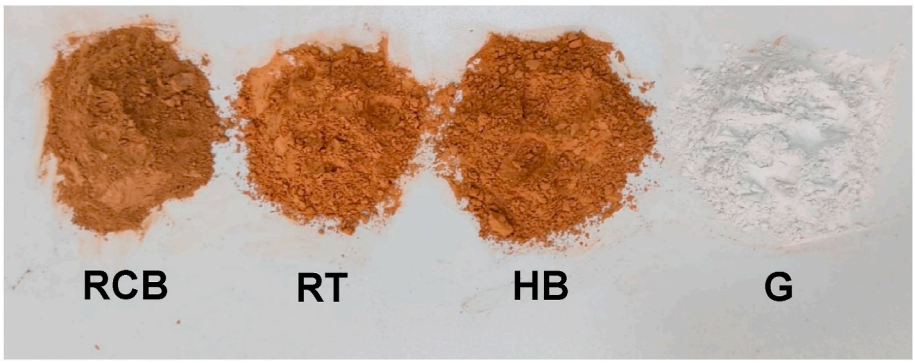

Fig. 2. Views of CDW-based precursors after milling.

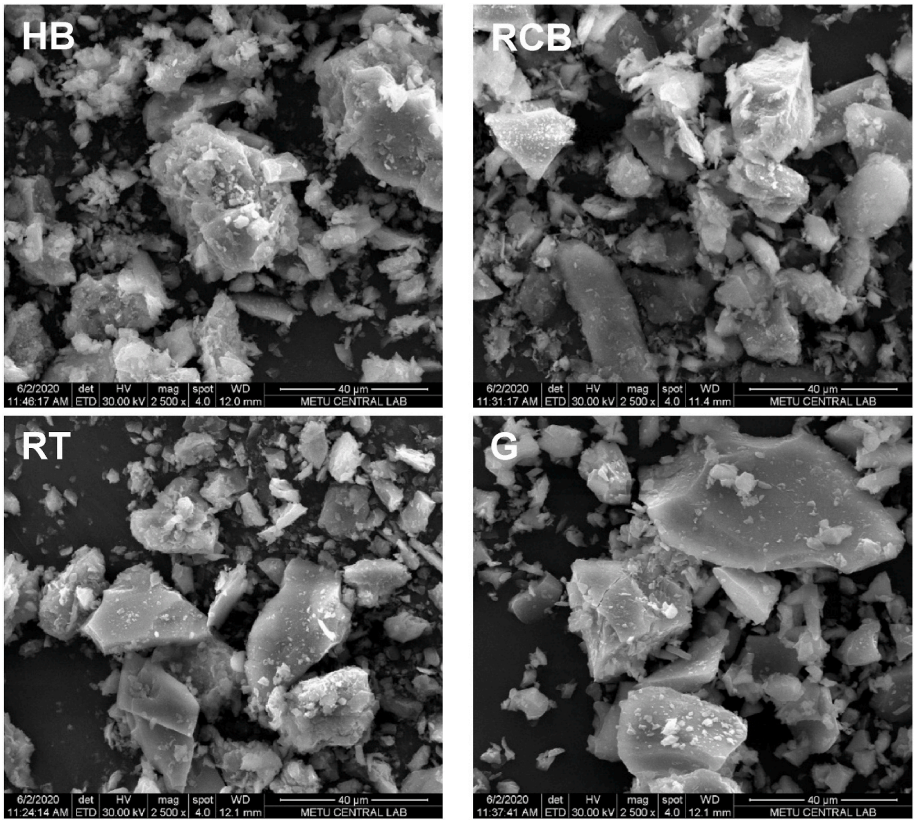

Fig. 3. SEM micrographs of CDW-based precursors.

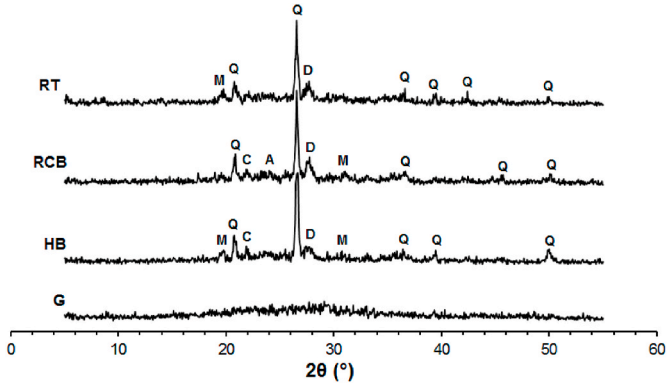

Fig. 4. XRD patterns of CDW-based precursors.

Table 2
Chemical formulations and powder diffraction file (PDF) numbers of crystalline phases in accordance with XRD analyses.

Crystalline phase	Symbol	PDF number	Chemical formula
Quartz	Q	96-101-1160	SiO_2
Crystobalite	C	96-900-8230	SiO_2
Diopside	D	96-900-5280	$Al_{0.6}CaMg_{0.7}O_6Si_{1.7}$
Mullite	M	96-900-5502	Al_2O_5Si
Akermanite	A	96-900-6115	$AlCa_2Mg_{0.4}O_7Si_{1.5}$

with the goal of finding an optimum alkaline activator that would not cause problems related to workability, rheological and mechanical properties. For all the mixtures produced, the water-to-precursor ratio was fixed at 0.33 and no chemical admixtures were added to better observe the sole effect of alkaline activators on geopolymerization. A suitable alkaline activator for the specified base mixture was chosen at

the beginning and the single use of NaOH as the alkaline activator was the initial focus. Following this, different alkaline activators were combined in certain proportions and the effects of their combined use on the rheological properties of the mixtures was investigated. One of the combinations was NaOH and $Ca(OH)_2$. Different amounts of $Ca(OH)_2$ were combined with NaOH to observe the effects of changing amounts of $Ca(OH)_2$ on the workability, rheological properties and compressive strength of the geopolymers. The addition of $Ca(OH)_2$ into low-calcium geopolymer systems provides features such as fast hardening and the ability to gain strength under ambient conditions and form calcium-based gel structures that contribute to strength [33]. Another activator combination was made using NaOH and Na_2SiO_3 to improve the mechanical performance by supporting the alkaline activation capacity of low-calcium precursors. From the knowledge acquired by using different alkaline activators in single and binary forms, geopolymers were produced with the ternary blends of NaOH, $Ca(OH)_2$ and Na_2SiO_3 and tested for workability, rheological properties and compressive strength.

The effects of different alkaline activators on the base mixture were observed using individual activators at fixed intervals. While using NaOH as the sole activator as the first step, the base mixture was activated by NaOH solutions with molarities of 5, 10, 15, 20, 25 and 30 M. However, initial results showed that molarities greater than 10 M resulted in high deviations of rheological parameters and inadequate flowability. The stickness of the geopolymer mixture became significant, especially for the NaOH molarity of 30 M. Thus, the range of NaOH molarities was limited to 5–15 M, with an increment rate of 1.25 M.

Although higher molarities (>10 M) of NaOH caused rheological problems, molarities higher than 10 M (up to 25 M with 5 M increments beyond 15 M) were still focused, considering the possible effects of other activators that may limit the detrimental effects of NaOH on the overall rheology of the base mixture. At the second stage, NaOH was combined with $Ca(OH)_2$ and Na_2SiO_3 separately to evaluate the effects of binary use of activators on rheological properties. $Ca(OH)_2$ was added to the NaOH-activated mixtures with ratios ranging from 2 to 10% of the total weight of precursors, with an increment rate of 2%. For mixtures with the binary use of NaOH and Na_2SiO_3, liquid-form Na_2SiO_3 was added to the NaOH-activated mixtures by 0.5 or 1.0 ratio of the weight of the solid flake-form NaOH. At the final stage, a ternary blend of all three activators was used in producing geopolymers. For the ternary use of activators, the optimal utilization rates obtained for different activators

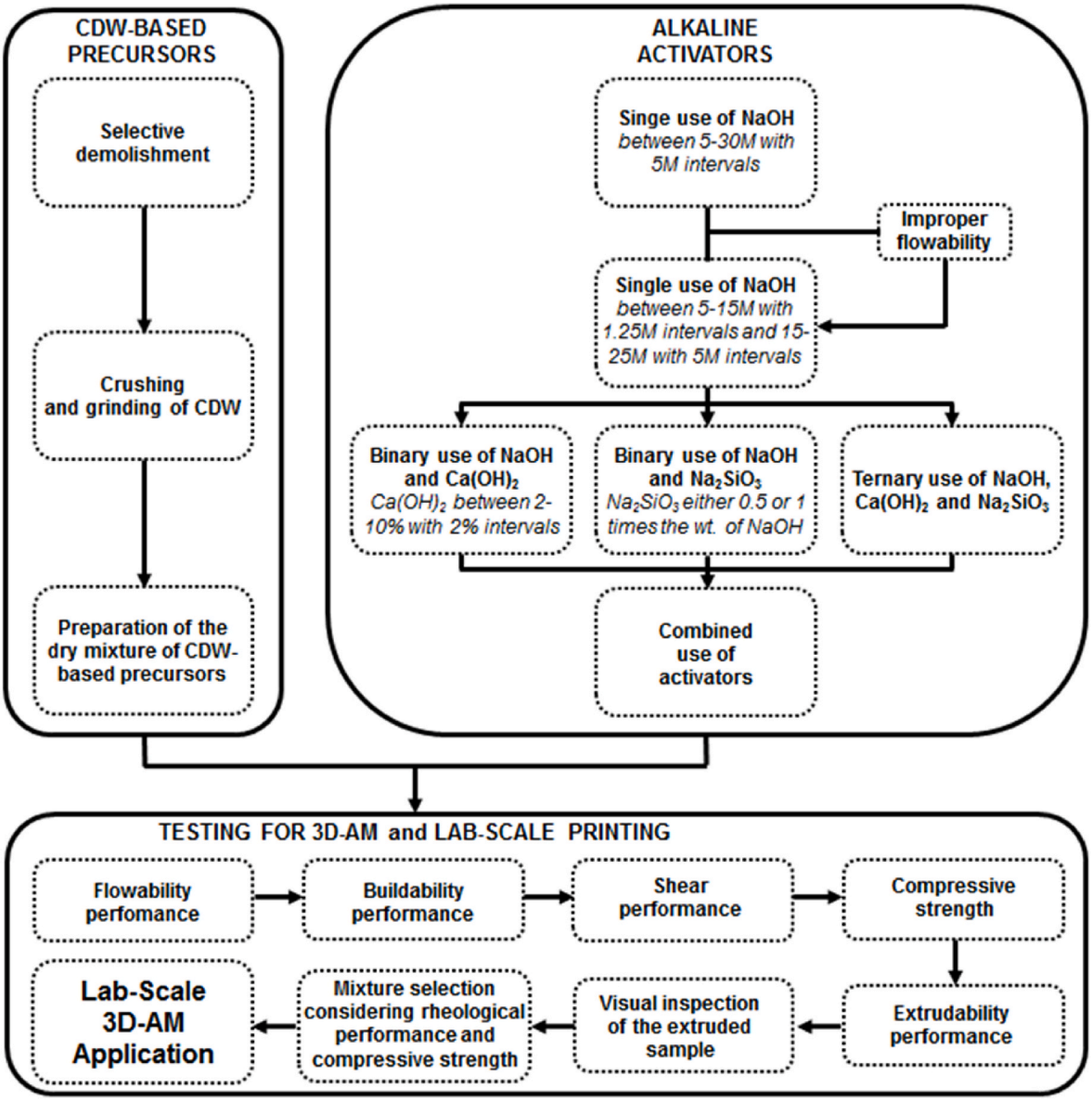

Fig. 5. Flowchart of the preparation, mixing and testing procedures.

from the previous two stages for single and binary use were used. Fig. 5 is a step-by-step flowchart explaining the work and Table 3 shows the mixture proportions of geopolymers tested in the study for clarity.

2.3. Mixing procedure

Geopolymer mixture preparation began with preparation of the activators. First, the solutions of NaOH-based alkaline activators were prepared by dissolving NaOH flakes in tap water to reach predetermined molarity levels. NaOH solutions were left to cool to room temperature before use, since the reactions between NaOH and water are exothermic and create high levels of heat. A standard mortar mixer was used during the preparation of the mixtures, and the mixing procedure included the following steps. CDW-based precursors were mixed for 1 min at low speed in dry conditions until obtaining desirable homogeneity. For the geopolymers including $Ca(OH)_2$ as the activator, precursors and Ca $(OH)_2$ powder were mixed together in this step. Then NaOH solution was slowly added into the precursors (with or without $Ca(OH)_2$ inclusion depending on mixture type) and mixing was continued at low speed for 1 min to ensure adequate distribution of the solution within the dry mixture. For the systems without Na_2SiO_3, mixing at low speed was continued for 90 s, followed by additional mixing at medium speed for 60 s before the completion of the mixing process. For systems incorporated with the binary (NaOH–Na_2SiO_3) and ternary (NaOH–Ca $(OH)_2$–Na_2SiO_3) use of alkaline activators, liquid Na_2SiO_3 was introduced into the NaOH-precursor slurry and the mixing of the wet slurry mixture was continued at low speed for 90 s, followed by additional medium-speed mixing for 60 s before the completion of the mixing process.

2.4. Testing

Materials used for 3D-AM purposes must have certain properties. Yield strength, which represents the capability of building layers on top of each layer, must be optimal to prevent deformation due to the load that will be exerted by the cast layers. Materials should not be too viscous to be extruded [34] but should have proper viscosity to achieve adequate mechanical characteristics simultaneously (Fig. 6). These properties therefore need to be balanced to obtain the most suitable materials for 3D-AM purposes (Fig. 6).

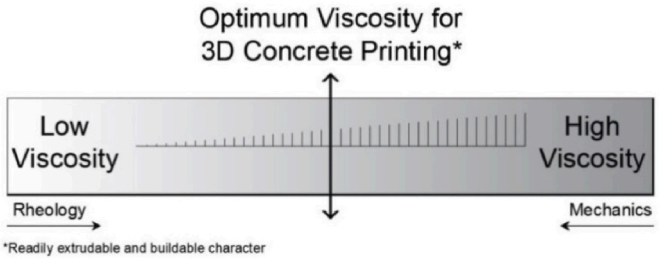

Fig. 6. Rheological and mechanical balance of materials with regard to viscosity (redrawn after [35]).

Table 3
Proportions of CDW-based geopolymer mixtures.

CDW-based precursor (1000 g)				Alkaline solution						Water-to-precursor ratio
RCB	RT	HB	G	$Ca(OH)_2$		NaOH (Molarity)	NaOH (g)		Na_2SiO_3 (g)	
				Rate (%)	Amount (g)					
300	300	300	100	0	0	5	66	Na_2SiO_3/NaOH	–	0.33
				2	20	6.25	82.5	= 0	–	
						7.5	99		–	
				4	40	8.75	115.5		–	
						10	132		–	
				6	60	11.25	148.5		–	
						12.5	165		–	
				8	80	13.75	181.5		–	
						15	198		–	
				10	100	20	264		–	
						25	330		–	
RCB	**RT**	**HB**	**G**	**$Ca(OH)_2$**		**NaOH (Molarity)**	**NaOH (g)**	Na_2SiO_3/NaOH	**Na_2SiO_3 (g)**	
				Rate (%)	**Amount (g)**			= 0.5		
300	300	300	100	0	0	5	66		33	
				2	20	6.25	82.5		41.3	
						7.5	99		49.5	
				4	40	8.75	115.5		57.8	
						10	132		66	
				6	60	11.25	148.5		N/A	
						12.5	165		N/A	
				8	80	13.75	181.5		N/A	
						15	198		99	
				10	100	20	264		N/A	
						25	330		N/A	
RCB	**RT**	**HB**	**G**	**$Ca(OH)_2$**		**NaOH (Molarity)**	**NaOH (g)**	Na_2SiO_3/NaOH	**Na_2SiO_3 (g)**	
				Rate (%)	**Amount (g)**			= 1		
300	300	300	100	0	0	5	66		66	
				2	20	6.25	82.5		82.5	
						7.5	99		99	
				4	40	8.75	115.5		115.5	
						10	132		132	
				6	60	11.25	148.5		N/A	
						12.5	165		N/A	
				8	80	13.75	181.5		N/A	
						15	198		198	
				10	100	20	264		N/A	
						25	330		N/A	

N/A: Not Applied

Along these lines, a series of tests were performed to evaluate the rheological properties and compressive strength of the geopolymers. Rheological properties were investigated by focusing mainly on the workability, buildability (shape-retention) and extrudability of the geopolymer mixtures. To represent the mechanical response, compressive strength measurements were made by using 50 mm-cube specimens of geopolymer mixtures. After preparation, mixtures were cast into pre-oiled cubic molds, where they stayed for 24 h with their surfaces covered. Following the initial 24 h, cubes were removed from their molds and subjected to further curing under laboratory conditions of 23 °C ± 2 and %50 ± 5 relative humidity until the completion of 7 and 28 days. Compressive strength results were found by taking the average obtained from six specimens for each proposed mixture and testing age. Tests performed to determine rheological properties are detailed in the following sections.

2.4.1. Flow table test

The flow table test was performed in accordance with the ASTM C1437-15 standard. Kazemian et al. [36] stated that there is a strong relationship between increased spreading diameter and yield stress. In this regard, "flowability index (Γ)", which takes the spreading diameters of the geopolymer mixtures into account, was determined. The following equation was used to calculate the flowability index by using the measured flow diameters of the geopolymer mixtures [37].

$$\Gamma = \frac{d_1 d_2 - d_0^2}{d_0^2}$$

where, d_0 is the inner diameter of the mold (100 mm), d_1 is the maximum spreading diameter and d_2 is the spreading diameter perpendicular to d_1 (Fig. 7).

2.4.2. Vane shear test

One of the key objectives of this study was to develop geopolymer mixtures with optimal flow properties suitable for 3D-AM technology. A vane shear test was performed to evaluate the flow properties of fresh geopolymers. This method has been applied successfully in the measurement of flow properties of fresh pastes and has been suggested for field use [38,39]. The test was conducted using a pocket-type vane shear tool (Fig. 8). The test determined the resistance of the material against the shear force and analyzed the rheological properties of the geopolymers. This method, which uses a single shear apparatus, was mainly used to compare the relative shear yield stresses of geopolymer mixtures, since specific yield stress values can vary as the stirrer or blade of the test apparatus and test methods change, regardless of adjustments [40].

Before the start of the test, the vane shear apparatus was positioned into the fresh mixture until the blades were fully immersed (Fig. 8). Then, a gradually increasing force was applied to the upper head of the apparatus in a clockwise direction until the blades at the lower end of the apparatus started to rotate freely. After free rotation occurred, the shear yield stresses of the mixtures were recorded from the indicator on the apparatus. In time, the mixtures started to lose their consistency due to setting, which affected extrudability characteristics and geopolymer quality after pumping in terms of the formation of pores, cracks, froth, etc. Therefore, in addition to the measurement performed right after mixture preparation, the vane shear test was repeated for time intervals of 30, 60 and 120 min to observe behavioral changes in shear yield stress with time and gain an understanding of the setting/workable time of the geopolymer mixtures.

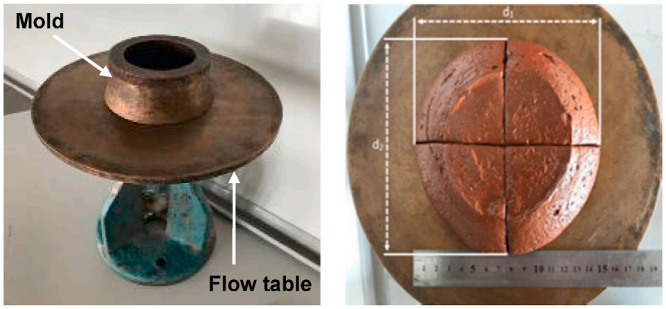

Fig. 7. Representative images showing the details of flow table test.

Fig. 8. Representative images showing the details of vane shear test.

2.4.3. Extrudability test

Extrudability is the capability of a material to be layered well in a line without deformation. A ram extruder was used in this study to determine the extrudability of geopolymers. The ram extrusion experiment is mostly perfomed on a laboratory scale to investigate extrusion flow and evaluate the rheological characteristics and extrudability of mixtures [41–44]. The ram extruder can be used to characterize the rheological behavior of dense cementitious mixtures, whose rheological response cannot be measured with rheometers ([45]). Ogura et al. [46] and Nerella et al. [47] used extrusion force to investigate the extrudability of materials and Figueiredo et al. [48] used a ram extruder to find their rheological parameters. Data obtained from the ram extruder was used in a Benbow-Bridgewater [49] model to reach the required rheological parameters. Later, Basterfield et al. [50] developed a new advanced model generated from the Gibson equation to describe the rigid-viscoplastic materials. This model was used by Zhou et al. [51] to study the rheological characteristics of short fiber-reinforced cement mortars. However, changes in the model continued and researchers developed a new ram extruder, advancing the model proposed by Basterfield et al. [50] and taking into account the contribution of shear stress on tapered surfaces [52]. On the other hand, according to Basterfield et al. [50] and Perrot et al. [52], the working principle of cementitious materials could be in accordance with the Von-Mises [53] criterion, which is about the distortion energy of the materials and is used to reach yielding of materials from the standard uniaxial test results. In this regard, elongational yield stress obtained from the ram extruder can be transferred into the shear yield stress, where materials started to flow. By using the equation below, relative shear yield stress of each mixture can be obtained to understand how the activator type/rate used influences the rheological response of the CDW-based geopolymers:

$$\tau_0 = \frac{\sigma_0}{\sqrt{3}}$$

where, τ_0 is the shear yield stress and s_0 is the elongational yield stress.

The ram extruder used in the current study was designed in accordance with several studies available in literature [45,51,54]. It consisted of four components: piston, chamber, nozzle and stands, details of which are shown in Fig. 9. The extruder was set up on a universal testing device capable of providing the required extrusion force. During the test, a

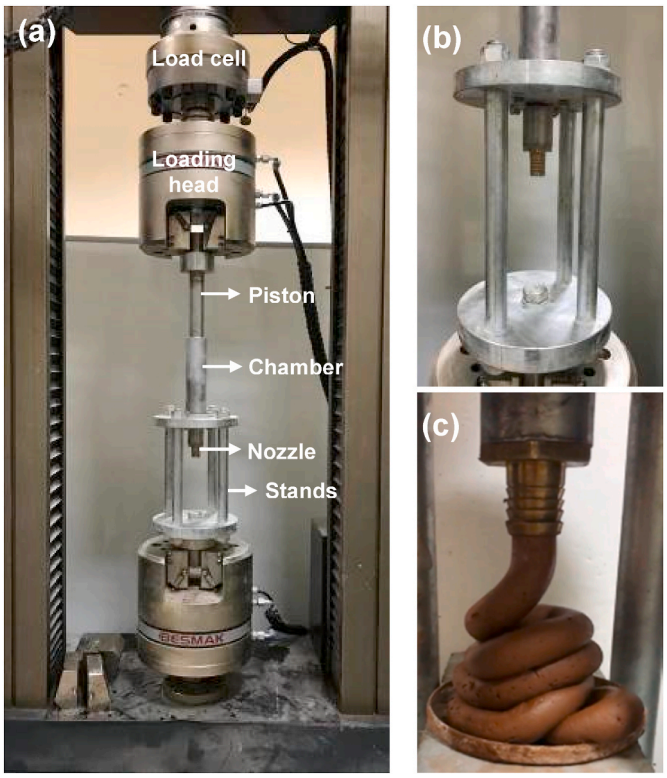

Fig. 9. (a) Overall view of the ram extruder, (b) closer view of the nozzle, (c) view during extrusion of CDW-based geopolymer.

piston speed of 2.25 mm/s was used to simulate the 3D-AM process at the lab scale, resulting in a flow speed of 16 mm/s because of the continuity equation (conservation of mass in pipeline). Although the diameter of the chamber where the piston moves was 4 cm, mixtures flowed through a 1.5 cm-diameter nozzle, which resulted in the differences between piston and flow speed. The speed of the piston was determined by taking the printing speed of the 3D printer designed by the authors into consideration, which was used in the final part of the work presented herein and can effectively work with the speed of 16 mm/s without causing problems related to the continuity of geopolymers during layering and incompatibility issues with the pump. Additionally, the distance between the nozzle and printing surface was shortened to prevent defects and rupture caused by tension increments in the mixtures due to extrusion from a large distance (Fig. 9-b,c).

The quality of the extruded materials was evaluated visually for the formation of defects, cracks, ruptures and holes. All tests were performed under the same laboratory conditions. Extrusion pressure was calculated by using the equation below, as also reported in the work of Chen et al. [45]:

$$\sigma_O = 4F/\pi \times D_0^2$$

where, σ_O represents the extrusion pressure or elongational yield stress when mixture flows, F is the corresponding average extrusion force recorded to achieve the preset piston speed and D_o is the inner diameter of the chamber, which is equal to 4 cm.

Since mixtures lose their consistency as a general response to progress in geopolymerization reactions, and this loss affects both extrudability characteristics and material quality after pumping, the time-dependent performance of the geopolymer mixtures was also investigated in terms of shear yield stress results measured by ram extruder after 30, 60, and 120 min from completion of initial mixing, similar to the vane shear test.

2.4.4. Buildability test

Buildability is the ability to perform additive manufacturing of mixtures without using formwork. It is essential for 3D-AM purposes since it offers an understanding of the layer-by-layer production technique in which each layer carries the extruded upper layer along with its own weight without shape change or collapse. Buildability is directly related to the viscosity and yield stress of mixtures. The higher the viscosity or yield stress, the better the buildability performance. However, there is a limit above which further increments in viscosity or yield stress lead to decreased extrudability performance, as the mixture gets significantly viscous. The literature includes a number of different test methods that have not yet been standardized for determination of buildability. This study used the testing method proposed by Nematollahi et al. [55]. The method is inspired by the mini-slump test method performed in accordance with the ASTM C1437 standard and modified to be compatible with the analysis of material behavior.

During the test, the mixture was placed in the mini slump cone as in flow table test. After a 1-min resting period, the cone was lifted up, a glass plate was placed on the fresh mixture and an additional weight was placed on the plate to evenly distribute the load. A static load of 600 g, including the weight of the glass plate, was applied for 1 min on the fresh sample. At the end of 1 min, the deformation of fresh geopolymer mixture was measured in two perpendicular directions by considering the final height of sample, and the average height was recorded (Fig. 10), since lower vertical deformation (slump) or higher final height means better buildability of the mixture under static loading.

3. Results and discussion

Geopolymerization is a complex process that takes place in more than one phase, beginning with the dissolution of the aluminosilicate precusors, continuing with the reactions between the precusors and activators and ending with condensation. These continuous activities largely depend on the type and dosage of the alkaline activators, as the activators are responsible for the dissolving and activation of the precursors, and contribute to changes in the rheological and mechanical properties of the ultimate geopolymeric material. Since different types and combinations of alkaline activators were used here, the results have beene discussed thoroughly, in accordance with the presence of different types of activators in geopolymer mixtures. As soon as the mixing process was completed, the abovementioned tests were performed in accordance with the single, binary and ternary use of activators, to examine the workability, rheological properties and compressive strength results of CDW-based geopolymer mixtures, details/discussions of which are provided in the following sections.

3.1. Effect of NaOH on rheological properties

Fig. 11 combines outcomes obtained of all tests evaluating the rheological response of geopolymer mixtures. It illustrates changes in the flowability index, buildability and vane shear stress results of geopolymer mixtures produced by NaOH of different molarities (ranging from 5 to 15 M with 1.25 M increments and from 15 to 25 M with 5 M

Fig. 10. Representative images showing details of the buildability test.

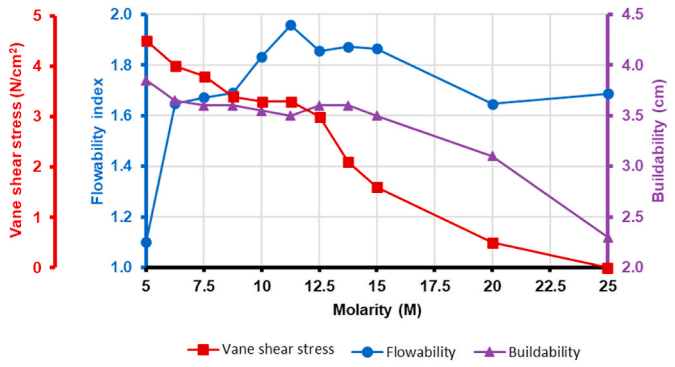

Fig. 11. Changes in the vane shear stress, flowability index and buildability of geopolymers produced by different molarities of NaOH solution.

increments). As seen from Fig. 11, flowability increased significantly when the molarity of NaOH solution was increased from 5 to 11.25 M. NaOH molarity from 11.25 M to 12.5 M showed decrements in flowability. Beyond 12.5 M, flowability stayed steady, with slight deviations up to 15 M. Dramatic decrements were observed at NaOH molarity of 20 M, while no considerable change was observed after 20 M. Shear yield stress results decreased continuously with increased molarity of the NaOH solution. A similar trend was also noted for buidability results, although the decremental behavior was slightly milder, especially up to an NaOH molarity of 15 M. Substantial decrements in the shear yield stress started to occur, especially after NaOH molarity of 11.25 M. Starting at 15 M, drops in shear yield stress values became significantly pronounced, instanteously flowing without exhibiting considerable resistance against the manually operated vane shear apparatus. This shows that mixtures with NaOH molarity of $\geq$15 M are not suitable for 3D-AM purposes, since reduced shear yield stress levels prevent geopolymer mixtures from maintaining stability after being extruded by the 3D printer. Moreover, buildability (an important parameter for 3D-AM, representing the capability to carry additional load caused by the extruded upper layer) decreased significantly after 15 M. Therefore, in the following sections of the study, where NaOH was used in combination with $Ca(OH)_2$ and Na_2SiO_3, NaOH molarities were selected to range from 5 to 15 M, with increments of 1.25 M. As noted previously, NaOH molarities between 11.25 M and 15 M were still taken into consideration, since the condition of the base geopolymer mixture was acceptable in regard to buildability and shear yield stress parameters for 3D-AM application. It was also factored in to consider the possible effects of other activators, which may limit the detrimental effects of high-molarity NaOH on the overall rheology of the base mixture.

The mechanism of geopolymerization must be carefully examined to better understand the influence of the NaOH concentration on the rheological properties of the mixtures. Geopolimarization reactions are composed of various dissolution and polycondensation events, where alkaline activators are used to provide a proper medium for the dissolution of precursors and the formation of final products [56,57]. After the initial dissolution of the precursors under a highly alkaline medium, oligomers start to form as a result of the reaction between the aluminosilicate monomers. In order to develop a 3-dimensional structure made out of SiO_4 and AlO_4 tetrahedral units, the already-formed oligomers initiate polycondensation reactions [9]. Considering that the individual steps of dissolution and polycondensation events occur due to the availability of the highly alkaline medium and are affected by the type and concentration of the alkaline activators, it can be stated that rheological and mechanical properties of the mixtures are in close relationship with the alkaline activators as well [58].

As mentioned above, an incremental trend in the flowability index implying enhancement in geopolymer workability was obvious up to an NaOH molarity of 11.25 M. This can be closely related to incremented in the dissolution rate of precursors with increased NaOH concentrations [59–61]. However, it was also observed that after an NaOH molarity of 11.25 M, flowability index results generally decreased up to 25 M. This may be due to significantly increased viscosity of NaOH solutions at higher molarities (higher than the 11.25 M threshold) decreasing overall flowability [58,62,63]. Another possible reason for lower flowability index results after exceeding the optimum NaOH molarity of 11.25 M is the limitations in the mobility of the ions as a result of the significant increments in the amount of ionic species in the mixtures [60,64]. Moreover, given the fact that most of the CDWs used in this study were clay-originated and clay has a layer-like structure, lower flowability results after 11.25 M can be related to the increased viscosity and stickiness of the geopolymers as a result of inter-particle friction coupled with the presence of a very high-molarity NaOH solution [65].

This differential behavior in flowability at different NaOH molarities was also observed visually during the flow table tests. Fig. 12, which shows representative views of the geopolymers produced using different NaOH molarities, with the excessive increments in NaOH molarity, geopolymers became significantly stickier and adhered both to the mold and flow table, with very low flowability.

A decrease was observed in buildability performance from an NaOH molarity of 5 M–6.25 M, however, and after that point, mixed buildability behavior was observed until 15 M with relatively small differences. Beyond 15 M, dramatic decrements in buildability started to be visible. Although buildability tests were performed at the fresh state, the results were very likely to have been affected by the stiffening of the geopolymer mixtures at the time of testing. The alkalinity of the medium should be in a range to provide proper dissolution and condensation [66]. It seems that until about an NaOH molarity of 15 M, dissolution of the precursors and the condensation reactions accelerated and the alkalinity of the geopolymer mixtures was suitable to provide proper stiffening of the geopolymers, resulting in higher buildability results. The decrements in the buildability after 15 M can be due to the restricting effect of higher NaOH molarity on geopolymerization [64]. Although the rate of dissolution increases at higher NaOH molarities, excessive presence of negatively charged monomers increases the repulsive forces between them. Under such conditions, monomers remain suspended in the pore solution until the attractive forces overcome the repulsive ones and promote the condensation [58]. This induces a delay in the condensation and therefore in the formation of stiff body, possibly lowering the buildability results.

The results presented in Fig. 11 appear contradictory: with the increases molarity of NaOH, both buildability and vane shear stress results decrease continuously while there are fluctuations in the flowability index results. These differences in the trends of different test results can be explained by the clear differences in the different testing methods. During the flowability index calculation, the flow table is dropped 25 times, which creates additional impact, forcing the fresh mixtures to flow. After exceeding a certain NaOH molarity level (11.25 M for this study), the stickiness of the mixture increases, and this decreases the flowability results despite the additional dropping impact. During buildability testing, however, a constant 600 g-static load was placed over the fresh sample for 1 min. With the placement of static load, decrements in buildability, with minimal changes up to around 15 M, were visible due to the anticipated effect of static load lowering the height of the fresh mixture. However, after 15 M, although the mixtures became sticky, static load caused height to decrease even more, given the delay in condensation reactions and the formation of stiff body. On the other hand, in the vane shear test, regardless of molarity and the condition of the fresh mixture, a slowly increasing force was applied to the apparatus until the lower end started to rotate freely. Beyond this free rotation movement, shear yield stress results were recorded. As mentioned above, when the molarity of the NaOH solution exceeded15 M, the formation of a rigid body of geopolymers was delayed, which in turn allowed the apparatus to freely rotate at much lower shear stress levels.

Results obtained in the presence of different NaOH molarities

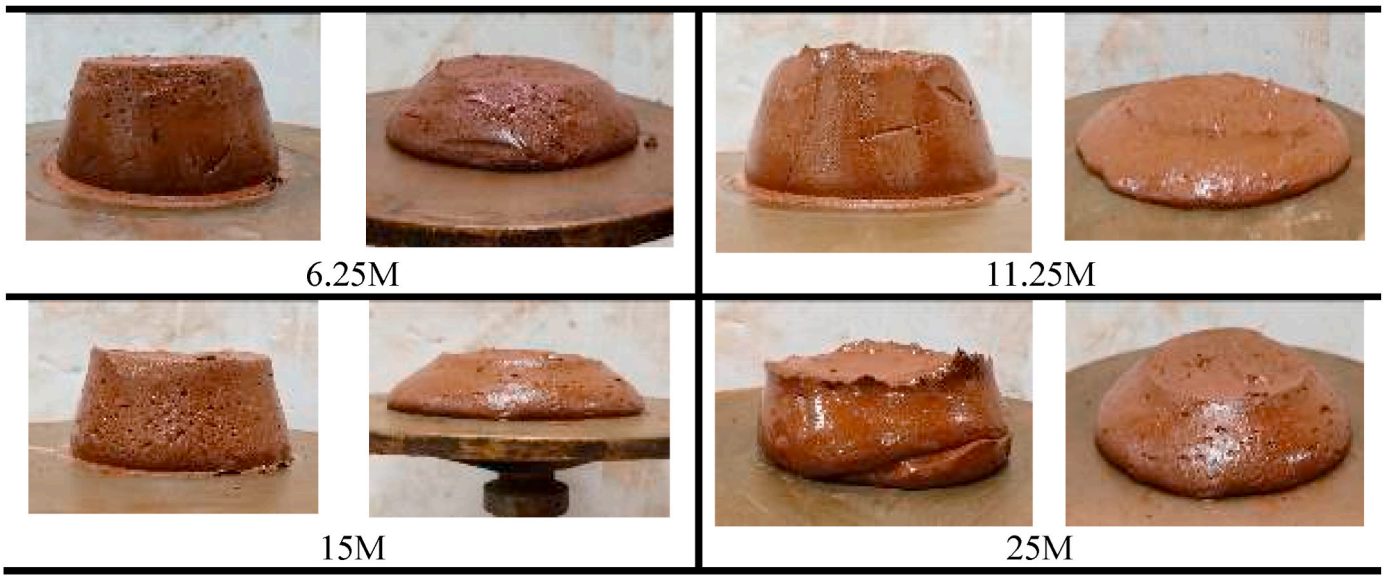

Fig. 12. Representative views of the geopolymer mixtures with different molarities of NaOH solution before and after the completion of flow table test.

indicate that the rheological properties of the geopolymer mixtures changed significantly at 6.25 M, although there were reasonable changes in the results with increased molarities of up to 11.25 M, and the mixtures were acceptable from the 3D-AM perspective. However, to avoid excessive amounts of NaOH use in geopolymer mixtures (which is undesirable for economic and occupational health and safety reasons), the NaOH molarity of 6.25 M was chosen for the ultimate mixture used for the laboratory-scale 3D printing, although different NaOH molarities were also used in subsequent sections of the work to see the effect of the combined use of activators on the rheological properties of the geopolymers.

3.2. *Effect of $Ca(OH)_2$ on rheological properties*

Fig. 13 shows buildability and flowability results of geopolymer mixtures with different molarities of NaOH solutions (5–15 M) and

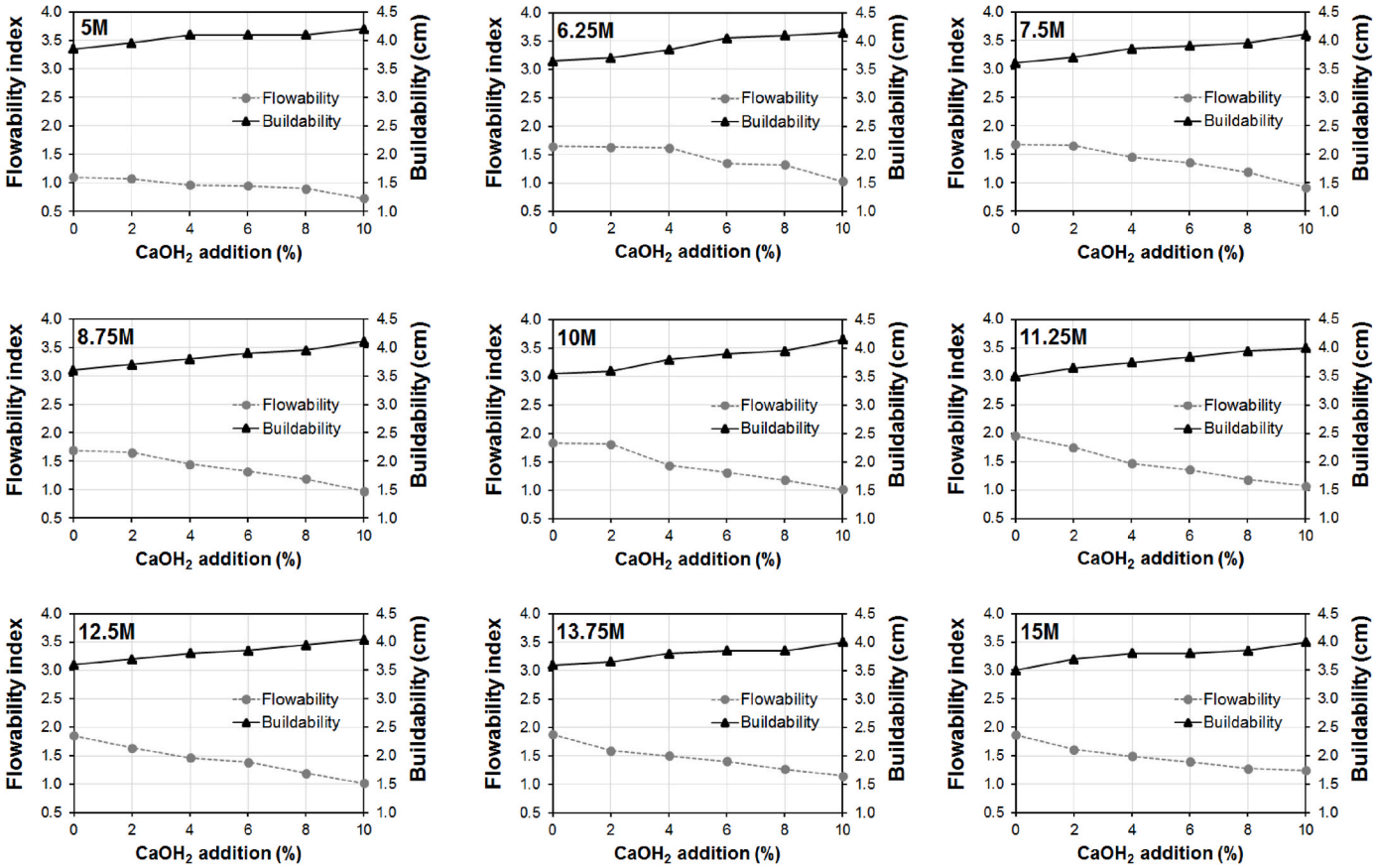

Fig. 13. Buildability and flowability results of mixtures for varying NaOH and $Ca(OH)_2$ rates.

$CaOH_2$ addition rates (0–10%). Vane shear stress results were also calculated right after the preparation of fresh mixtures and 30, 60 and 120 min after to observe behavioral changes in shear yield stress with time (Table 4).

As the $Ca(OH)_2$ addition rate was increased in geopolymer mixtures, the flowability index decreased, irrespective of NaOH molarity (Fig. 13). There are several reasons for this behavior. The availability of $Ca(OH)_2$ in geopolymer systems has been reported to favor the formation of reaction products that provide rigidity to the paste [67]. $Ca(OH)_2$ is very likely to react with the dissolved silicates and aluminates to form C–S–H and C-A-S-H gels, which can increase geopolymer rigidity [33,68–70]) and therefore decrease flowability. Water content is very important for flowability [71,72]. With increased increments in the rate of $Ca(OH)_2$, the powder content in the mixtures increases and water-to-solid ratio decreases, and flowability results decrease as well. Increased amounts of $Ca(OH)_2$ also lead to an increase in Ca^{2+} ions, which exhibit stronger

Table 4
Time-dependent vane shear stress results of geopolymer mixtures with different combinations of alkaline activators.

Na_2SiO_3/NaOH		0				0.5				1			
NaOH (M)	$Ca(OH)_2$ (%)	Vane shear stress (N/cm^2)				Vane shear stress (N/cm^2)				Vane shear stress (N/cm^2)			
		0min	30min	60min	120min	0 min	30min	60min	120min	0min	30min	60 min	120min
5	0	4.5	4.7	5.4	9.0	5.0	8.0	9.6	/	5.1	8.1	/	/
	2	4.5	4.9	5.9	9.2	5.2	8.1	9.6	/	5	8.1	/	/
	4	4.7	5.3	5.9	9.3	6.3	8.9	9.7	/	8.5	9.5	/	/
	6	5.4	5.6	6.0	9.5	8.3	9.6	/	/	8.7	9.6	/	/
	8	5.5	5.6	6.2	9.5	9.1	9.5	/	/	8.7	9.5	/	/
	10	5.7	6.0	6.7	9.6	9.0	9.6	/	/	8.9	/	/	/
6.25	0	4.0	4.5	6.3	8.5	3.0	8.3	/	/	2.8	8.7	/	/
	2	4.2	5.9	7.1	8.9	3.2	8.6	/	/	2.9	8.9	/	/
	4	4.6	6.4	8.0	8.7	3.3	8.8	/	/	3.1	9.4	/	/
	6	5.5	6.9	8.1	9.6	3.7	8.9	/	/	3.2	/	/	/
	8	5.4	6.8	8.2	9.1	5.0	9.0	/	/	3.4	/	/	/
	10	5.5	7.1	8.8	9.5	6.5	9.1	/	/	3.6	/	/	/
7.5	0	3.8	4.5	4.9	6.9	1.4	9.7	/	/	2.4	9.4	/	/
	2	4.1	4.5	5.7	6.5	1.2	9.7	/	/	2.5	9.5	/	/
	4	4.0	4.7	6.0	7.3	1.3	9.6	/	/	2.4	9.4	/	/
	6	4.2	4.9	6.1	7.5	1.4	9.6	/	/	2.8	/	/	/
	8	4.5	5.1	6.0	7.8	1.3	/	/	/	2.9	/	/	/
	10	5.2	6.1	7.3	8.6	1.8	/	/	/	3.3	/	/	/
8.75	0	3.4	4.0	4.5	5.5	1.4	9.6	/	/	1.8	9.6	/	/
	2	3.5	4.1	4.8	5.9	1.2	9.6	/	/	1.9	9.6	/	/
	4	3.5	4.0	4.8	6.0	1.2	9.6	/	/	2.1	9.5	/	/
	6	3.6	4.1	4.9	6.2	1.3	9.6	/	/	2.3	/	/	/
	8	3.9	4.3	5.2	6.0	1.4	9.6	/	/	2.4	/	/	/
	10	4.2	4.8	5.7	6.9	1.5	/	/	/	2.6	/	/	/
10	0	3.3	4.0	4.5	5.3	0.6	5.3	/	/	1.4	5.5	/	/
	2	3.2	4.1	4.8	5.5	0.8	7.0	/	/	1.5	6.5	/	/
	4	3.3	4.2	5.1	5.7	1.0	8.0	/	/	1.8	7.3	/	/
	6	3.3	4.1	5.1	5.8	1.2	9.6	/	/	1.7	/	/	/
	8	3.3	4.2	5.2	6.1	1.3	9.5	/	/	1.6	/	/	/
	10	4.0	4.9	5.8	6.6	1.4	/	/	/	2.1	/	/	/
11.25	0	3.3	4.0	4.8	5.4	N/A	N/A	N/A	N/A	N/A	N/A	N/A	N/A
	2	3.3	4.1	4.9	5.7	N/A	N/A	N/A	N/A	N/A	N/A	N/A	N/A
	4	3.5	4.2	5.0	6.0	N/A	N/A	N/A	N/A	N/A	N/A	N/A	N/A
	6	3.5	4.2	4.8	5.9	N/A	N/A	N/A	N/A	N/A	N/A	N/A	N/A
	8	3.6	4.3	5.1	6.1	N/A	N/A	N/A	N/A	N/A	N/A	N/A	N/A
	10	3.9	4.9	5.8	6.5	N/A	N/A	N/A	N/A	N/A	N/A	N/A	N/A
12.5	0	3.0	3.8	4.7	5.6	N/A	N/A	N/A	N/A	N/A	N/A	N/A	N/A
	2	3.5	4.0	4.8	5.8	N/A	N/A	N/A	N/A	N/A	N/A	N/A	N/A
	4	3.6	4.0	4.9	6.0	N/A	N/A	N/A	N/A	N/A	N/A	N/A	N/A
	6	3.4	3.9	4.9	5.9	N/A	N/A	N/A	N/A	N/A	N/A	N/A	N/A
	8	3.6	4.4	5.2	6.1	N/A	N/A	N/A	N/A	N/A	N/A	N/A	N/A
	10	4.0	5.0	5.9	7.1	N/A	N/A	N/A	N/A	N/A	N/A	N/A	N/A
13.75	0	2.1	3.2	4.8	5.0	N/A	N/A	N/A	N/A	N/A	N/A	N/A	N/A
	2	3.1	3.8	5.0	5.8	N/A	N/A	N/A	N/A	N/A	N/A	N/A	N/A
	4	3.2	3.9	5.1	6.0	N/A	N/A	N/A	N/A	N/A	N/A	N/A	N/A
	6	3.3	4.0	4.9	6.1	N/A	N/A	N/A	N/A	N/A	N/A	N/A	N/A
	8	3.5	4.1	4.6	5.9	N/A	N/A	N/A	N/A	N/A	N/A	N/A	N/A
	10	3.9	4.7	5.8	6.9	N/A	N/A	N/A	N/A	N/A	N/A	N/A	N/A
15	0	1.6	2.3	3.0	4.0	0.5	5.2	6.9	7.9	0.6	6.5	9.2	/
	2	2.5	3.0	3.6	4.3	0.5	7.0	7.8	8.2	0.5	6.4	9.2	/
	4	2.5	3.1	3.5	4.5	1.0	7.2	7.6	8.1	0.9	7.0	9.6	/
	6	3.2	3.6	4.1	4.7	1.4	7.0	7.6	8.3	1.0	7.5	/	/
	8	3.1	3.8	4.2	4.6	1.4	7.5	7.9	8.4	1.0	8.1	/	/
	10	3.2	4.0	4.4	4.9	1.5	7.4	8.1	8.8	1.3	8.4	/	/

N/A: Not applied.
/: Test could not be conducted (exceed the capacity of test equipment).

electrostatic attraction and charge neutralization followed by accelerated geopolymerization [73] and decreased flowability results. In addition, the availability of the OH^- ions in the presence of increased amounts of $Ca(OH)_2$, can cause the formation of a large number of active groups that lead to rapid geopolymerization and lower flowability [74].

It is important to note that when mixtures were produced solely with NaOH as the alkaline activator, there were drops in the flowability results with increased molarity levels (>11.25 M) due to the increased stickiness of the mixtures to the mold and flow table. As a clear beneficial effect, no drops in flowability results were observed when NaOH was combined with the $Ca(OH)_2$, and irrespective of the rate of $Ca(OH)_2$ addition, stickiness decreased significantly. In terms of buildability performance, as the $Ca(OH)_2$ addition rate was increased in geopolymer mixtures, general increments in buildability results were recorded (Fig. 13). This was an expected outcome, since dissolved $Ca(OH)_2$ takes part in the production of C–S–H and C-A-S-H gels [75], which are strength-giving reaction products that increase the rigidity, density, and therefore the load-bearing capacity of the mixtures [33,68,76].

Table 4 shows the vane shear stress results at the end of different time intervals for geopolymers produced with different combinations of alkaline activators. The vane shear stress results of the geopolymers with different combinations of NaOH and $Ca(OH)_2$ can be followed from the first column, where Na_2SiO_3/NaOH is zero. Right after initial mixing and testing (0 min), a clear incremental trend in the vane shear stress results was observed with increased $Ca(OH)_2$ addition rates for a given NaOH molarity. This result was expected, given the fact that the increased use of $Ca(OH)_2$ resulted in increments in rigidity [67], lowered the water-to-solid ratio [71,72] and triggered colloidal interactions in the geopolymer mixtures [77], all of which increased the endurance of the mixtures to hold additional shear forces.

Vane shear stress tests were also performed 30, 60 and 120 min after initial mixing of the geopolymers to get an idea about their open-time workability, which is a critical parameter for 3D-AM applications (Table 4). For mixtures with binary blends of different amounts of NaOH and $Ca(OH)_2$, irrespective of the utilization rate of alkaline activators, vane shear stress results increased with time. These increases may be correlated with changes in the setting time of geopolymer mixtures, as enhancements in setting would lead to increments in vane shear stress levels.

Chen et al. [78] concluded that for metakaolin-based geopolymers with external Si content (similar to those used here, with mixtures including CDW-originated combined clay- and glass-based precursors), the presence of calcium could substantially accelerate setting. The acceleration in setting is explained by the promotion of geopolymer gel formation in the presence of calcium, rather than the formation of C-A-S-H gels, which were reported not to be directly involved in setting. This is explained by the protective-layer mechanism, which states that calcium promotes the dissolution of the precursor since it consumes Si in the solution and reduces the probability of the formation of a protective layer of geopolymer gel around the precursor particles and the inhibition of dissolution capacity [78]. Considering the further time-dependent developments in the geopolymer gel formation in the presence $Ca(OH)_2$, increments in the vane shear stress results with time may be explained. To sum up, when NaOH was combined with $Ca(OH)_2$ in geopolymer mixtures, an open workable time of at least 2 h was acquired regardless of activator utilization rate, which is critical for 3D-AM applications in real field conditions.

3.3. Effect of Na_2SiO_3 on the rheological properties

Na_2SiO_3 ratios were determined as certain multiples of the amount of NaOH used and added at 0.5 and 1 times the weight of NaOH to the mixtures. Since workability generally exhibited poor performance after an NaOH molarity of 10 M and suitable rheology for 3D-AM purposes could not be obtained, no detailed investigations for NaOH molarities higher than 10 M were made. However, to have an understanding of the effect of high NaOH molarity on rheological response, a single geopolymer mixture with 15M-NaOH solution was produced and tested in the presence of other types of alkaline activators. The flowability index, buildability and vane shear stress results of geopolymers with binary and ternary blends of different alkaline activators are shown in Table 4, Fig. 14 and Fig. 15.

The effect of combined NaOH and Na_2SiO_3 on flowability, buildability and vane shear stress results can be determined by comparing the data in Fig. 13 with Figs. 14 and 15 and Table 4. Mixtures activated with binary blends of NaOH and Na_2SiO_3 showed increased flowability with the use of Na_2SiO_3 for each NaOH molarity, even though Na_2SiO_3 has very high viscosity [79,80]. These increments in flowability can be explained by the increments in the aqueous solution content with the addition of liquid Na_2SiO_3 [71,72,80]. Significant drops in buildability performance were observed with the addition of Na_2SiO_3 for a given molarity of the NaOH solution, most likely due to the increased liquidity of the mixtures. Excluding the NaOH molarity of 5 M, vane shear stress results decreased with the use of Na_2SiO_3. This exception may be due to fact that when 5M-NaOH was used, the mixture was in its stiffest state compared to other NaOH molarities and the Na_2SiO_3 amount did not compensate for this stiffness. With time, vane shear stress results increased as a result of the progression in the geopolymerization reactions. In Table 4 either "/" or "N/A" signs were used for time-dependent changes in vane shear stress results. "/" means vane shear apparatus could not perform any measurement, as the consistency of mixtures exceeded the capacity of the measurement devices. "N/A" stands for "Not Applied," meaning that vane shear stress testing was not performed due to anticipated unsuitable consistency/viscosity for 3D-AM purposes. With the use of Na_2SiO_3, the open-time performance of mixtures decreased suddenly and the workable time period of the fresh mixtures was limited to 60 min for each NaOH molarity except 15 M. This shortening in the open-time period can be related to advancements in geopolymerization reactions due to the reactive soluble silica content of Na_2SiO_3 [81–83]. However, at the considerably higher alkalinity of 15 M, formation of repulsive forces resulting from negatively charged ions could hinder geopolymerization [60,64] and extend the open-time period. Moreover, as the liquid/solid ratio increases, setting time may also increase since extra water tends to dilute the concentration of alkali-activated solution, delay the alkali-activation rate and extend the setting time [84,85].

When mixtures were incorporated with the ternary blend of NaOH, $Ca(OH)_2$ and Na_2SiO_3, flowability results exhibited a general incremental trend regardless of the Na_2SiO_3/NaOH ratio, except NaOH molarities of 5 and 6.25 M. At lower NaOH molarities, leaching of Ca ions is more favored [62,86] and addition of Na_2SiO_3 increases the amount of active Si. As a result, dissolved Ca and Si ions may react and form increased amounts of C–S–H and C-A-S-H gels [68–70,81–83,87], which may explain decrements in flowability results at lower molarities of NaOH. An opposite case to what was explained above, paired with the beneficial effects of Na_2SiO_3 addition in increasing fluidity [71,72,80], can lead to increments in the flowability results.

Buildability results were adversely affected by the presence of Na_2SiO_3 in geopolymer mixtures. For each NaOH molarity, lower buildability results were recorded irrespective of the amount of $CaOH_2$ available, most probably due to increased liquid/solid ratios reached when Na_2SiO_3 was used (Figs. 13–15). Furthermore, utilization of Na_2SiO_3 led to decrements in vane shear stress results for all NaOH molarities, except 5 M. When timely changes in vane shear stress results are considered, it can be concluded that the rigidity gain of geopolymers was much faster for mixtures with ternary blends of alkaline activators showing the clear effect of Na_2SiO_3. Open-time of mixtures incorporated with the ternary use of alkaline activators ranged from 30 to 60 min, and most of the mixtures lost their workability in a very short period of time. For mixtures with a Na_2SiO_3/NaOH ratio of 1, workability was lost in a much shorter period of time that those with a Na_2SiO_3/NaOH ratio of 0.5 (Table 4). As the possible reasons for the observed behaviors were

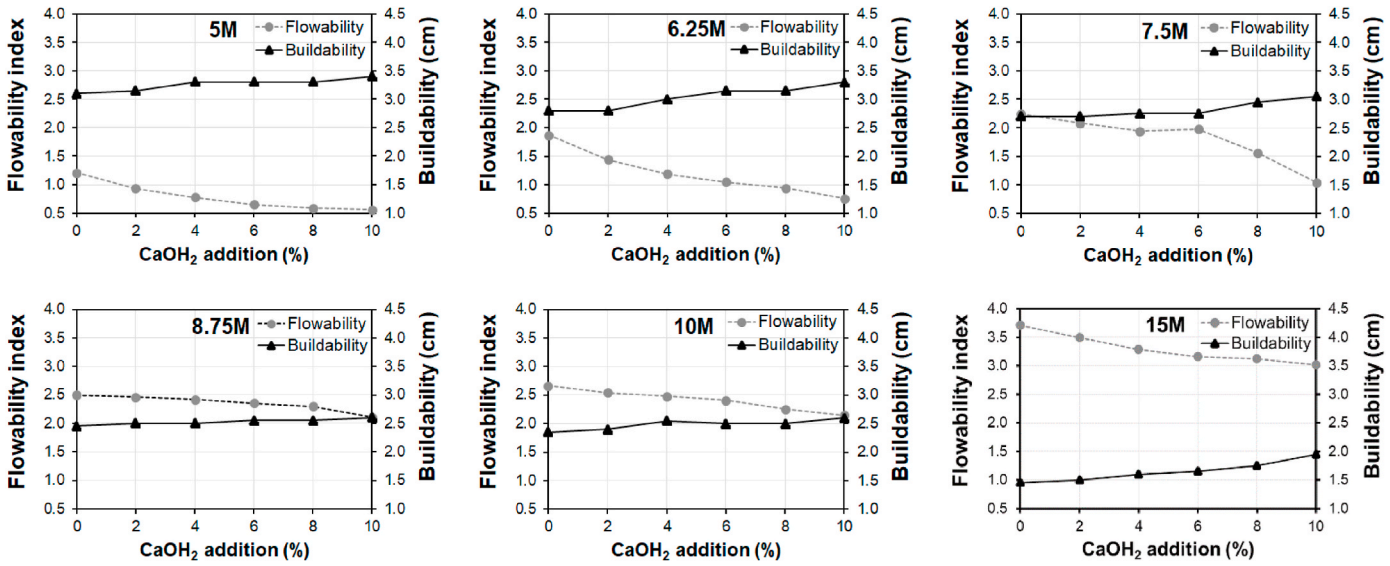

Fig. 14. Buildability and flowability results of the mixtures for varying NaOH and $Ca(OH)_2$ rates with Na_2SiO_3/NaOH of 0.5.

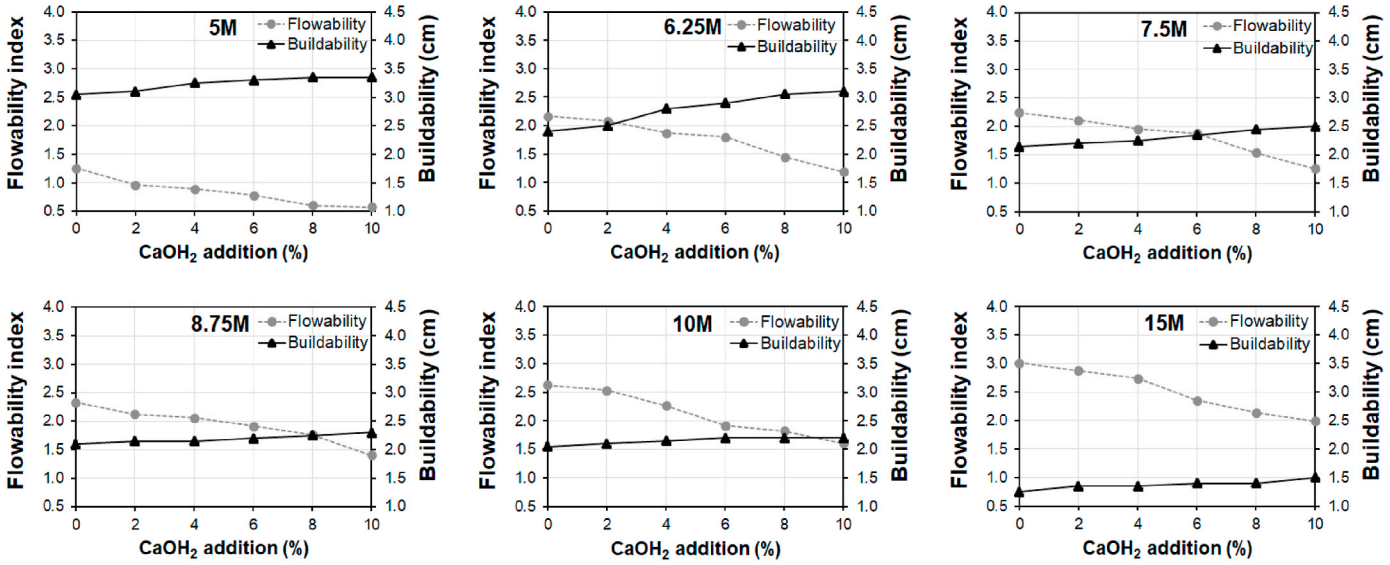

Fig. 15. Buildability and flowability results of the mixtures for varying NaOH and $Ca(OH)_2$ rates with Na_2SiO_3/NaOH of 1.

explained earlier, no further discussion is made here.

3.4. Effect of different alkaline activators on compressive strength

Table 5 shows the average compressive strength results of geopolymer mixtures developed using different combinations of alkaline activators. Geopolymers activated by the single use of NaOH and binary use of NaOH and $Ca(OH)_2$ could not develop remarkable strength when the molarity of NaOH was higher than 10 M. In addition, in the case of mixtures with Na_2SiO_3, no evaluation was made for those with NaOH molarities between 10 and 15 M. Therefore, these results are not included in Table 5.

When the molarity of NaOH was increased from 5 to 6.25 M, general increments in the compressive strength results were observed. The results for mixtures activated by 7.5M-NaOH were similar to those activated by 6.25M-NaOH. After an NaOH molarity of 7.5 M, results gradually decreased. For this case, increments in compressive strength are attributed to the increased rate of dissolution of precursors [59–61], while decrements are attributed to the restricted mobility of the ions as a result of the repulsion between them hindering geopolymerization at high alkalinity [58,60,64]. The highest average compressive strength obtained with the sole use of NaOH was 10.8 MPa at the end of 28 days ambient curing, which has been defined as "low" by researchers and led us further modify the mixture compositions with further combinations of alkaline activators for improved strength.

For a given NaOH molarity, increments in the amount of $Ca(OH)_2$ caused compressive strength results to increase, most likely due to formation of additional C-A-S-H and N-A-S-H gels [68–70,88] and the formation of a large number of active groups accelerating the geopolymerization process [73,74]. Moreover, addition of calcium sources to the system increased the strength under ambient curing conditions [33]. However, for 15M-NaOH, mixtures could not develop any strength since $Ca(OH)_2$ is incapable of being solved at very high alkalinity [86], and therefore, the precipitated $Ca(OH)_2$ becomes unable to react with the precursors [69]. The effects of NaOH molarity on the compressive strength results of mixtures in which $Ca(OH)_2$ was used as the second activator were similar to the trend observed for mixtures with only NaOH. Geopolymers activated by the binary use of NaOH and $Ca(OH)_2$

Table 5
Average compressive strength results (MPa) of geopolymers activated by different combinations of alkaline activators cured under ambient condition.

Na_2SiO_3/NaOH		0		0.5		1	
NaOH (M)	$Ca(OH)_2$ (%)	7 days	28 days	7 days	28 days	7 days	28 days
5	0	5.7	9.7	5.7	7.1	6.2	8.5
	2	7.6	11.2	7.6	11.8	7.6	10.9
	4	7.6	12.7	7.7	15.0	6.3	11.6
	6	8.0	13.7	7.8	16.7	13.9	17.8
	8	8.3	14.7	9.1	18.8	10.9	16.7
	10	8.1	15.1	9.9	19.7	11.3	17.1
6.25	0	5.9	10.5	5.7	7.0	5.6	7.8
	2	7.6	9.9	6.6	9.7	6.3	8.7
	4	7.7	11.9	8.0	17.9	8.1	9.9
	6	7.4	11.8	8.5	19.2	14.7	23.0
	8	8.1	13.9	7.3	17.5	13.0	19.9
	10	7.6	16.4	7.0	16.8	14.1	19.5
7.5	0	5.7	10.8	5.7	6.4	7.0	8.5
	2	6.3	10.4	6.6	13.4	8.7	9.1
	4	7.6	11.2	8.0	17.1	9.2	14.6
	6	6.2	12.7	8.7	19.7	10.8	20.6
	8	6.3	16.8	8.4	18.8	12.7	19.0
	10	5.9	13.4	9.4	18.5	13.6	20.2
8.75	0	5.6	8.8	–	5.9	7.0	7.8
	2	5.7	9.4	6.2	8.5	7.3	7.8
	4	6.2	10.1	7.0	13.9	10.5	13.4
	6	5.7	13.4	8.1	18.2	11.9	15.8
	8	5.7	12.6	7.8	17.8	10.9	16.8
	10	5.7	13.4	9.0	22.1	12.0	17.8
10	0	5.7	8.7	6.0	6.6	6.4	7.7
	2	5.6	7.0	7.8	8.5	6.4	8.8
	4	5.7	8.5	9.1	13.3	6.7	9.4
	6	5.6	11.1	12.2	16.7	11.8	13.0
	8	5.7	11.3	10.2	17.5	9.2	16.4
	10	6.3	12.3	8.1	19.3	7.7	18.8
15	0	–	–	–	5.7	5.9	7.4
	2	–	–	–	5.9	6.2	8.5
	4	–	–	–	7.1	5.7	9.5
	6	–	–	–	7.7	6.9	13.9
	8	–	–	–	7.6	6.6	13.4
	10	–	–	–	8.0	7.0	16.0

exhibited a maximum compressive strength of 16.8 MPa at the end of 28 days of ambient curing.

When Na_2SiO_3 was used in combination with NaOH for a given NaOH molarity, all compressive strength results showed a decreasing trend except 15M-NaOH. These decrements were attributed to the increased liquidity of the mixtures, which led to the formation of a more porous structure. In addition, the CDW-based precursors included significant amounts of Si, and providing extra Si to the system with the addition of Na_2SiO_3 may have led to coagulation of silica and faster setting, which does not allow for homogenous mixing, resulting in poor and incipient polymerization [9,10]. When Na_2SiO_3 was used in combination with the NaOH and $Ca(OH)_2$ collectively, compressive strength results increased with the higher $Ca(OH)_2$ amounts. Possible causes for this behavior have been explained previously. Mixtures incorporating the ternary blend of alkaline activators cured under ambient conditions resulted in 28-day compressive strength results of 22.1 and 23.0 MPa for Na_2SiO_3/NaOH ratios of 0.5 and 1, respectively. No considerable influence of Na_2SiO_3/NaOH ratio on the compressive strength results was observed.

The compressive strength results obtained after 28 days may seem low compared to traditional concretes produced with ordinary Portland cement, especially for structural use, although these strength levels are adequate for non-structural use. However, it is of great importance to note that no special attention was paid here to increase the compressive strength results of geopolymer mixtures. since the main focus of this study was to investigate the effect different alkaline activators and their single, binary and ternary combination effects on the rheological properties of CDW-based geopolymers. There are several ways to do this, such as increasing the fineness of CDW-based precursors, using conventional mineral admixtures in combination with CDW, applying high curing temperature, etc. to increase the compressive strength capacity of geopolymers. Some of these methods are considered energy-inefficient and inapplicable, especially for the 3D-AM purpose, which was the main purpose of the current research.

3.5. Extrudability analysis

For 3D-AM purposes, one of the most important characteristics of a mixture is its extrusion capability, which is the ability to be pumped from a nozzle with the lowest energy consumption, and conveying easily and reliably from the delivery system. Before starting the 3D printing application at laboratory-scale, rheological property (i.e. adequate flowability, higher buildability, appropriate initial vane shear stress and longer open-time period) and compressive strength results of geopolymer mixtures were taken into consideration for a final mixture design suitable to work with the ram extruder. Consequently, mixtures activated with the binary use of NaOH molarity of 6.25 M together with $Ca(OH)_2$ amounts of 6, 8 and 10% were tested with the ram extruder to select the mixture to be used for laboratory-scale 3D-printing. Mixtures with Na_2SiO_3 were not tested with the ram extruder since they exhibited lower buildability and considerably low workable time, as explained in the previous sections.

Table 6 shows the time-dependent shear yield stress results of geopolymer mixtures tested by the ram extruder. Increments in the shear yield stress results were observed with the increase in $CaOH_2$ addition rate. Since the sensitivity of the vane shear test was much lower than the ram extruder, such increments were not observed in the vane shear test results. With time, the shear yield stress results of the mixtures increased due to the progression in geopolymerization as observed by vane shear test, yet the effects of $CaOH_2$ addition (6–10%) on the reaction rate were not as evident as in the vane shear test. (As these subjects have already been discussed in detail, they are not further discussed here.) Each mixture had an open-time period of at least 120 min, as mixtures are extrudable via ram extruder with that amount of time.

Fig. 16 shows the extruded samples at 0, 30, 60 and 120 min after mixing. Visual examinations of the samples looked at cohesion and continuity of the materials, the ability of mixtures to be extruded continuously with the geometry of the nozzle without any disintegration and clogging, and analyzed the formation of cracks and/or splitting. As shows in Fig. 16, in terms of defects and continuity of the extruded mixture, all mixtures were similar, although fewer defects and better continuity were observed for the mixture with 6.25M-NaOH and 10% $Ca(OH)_2$, regardless of the testing period (Table 6). Although this mixture exhibited the highest shear yield stress, when the higher compressive strength of this mixture was taken into account, it was chosen for the laboratory-scale 3D printing application.

3.6. 3D-AM application at laboratory scale

3D-AM is a complex and interconnected process. The properties of the materials, printing speed, nozzle shape and flow rate all have a significant effect on the quality of printed materials [24,89], although

Table 6
Time-dependent shear yield stress results (N/mm^2) of geopolymer mixtures as determined by the ram extruder.

NaOH (M)	$Ca(OH)_2$ (%)	Shear yield stress			
		0 min	30 min	60 min	120 min
6.25	6	0.297	0.595	0.814	1.145
	8	0.329	0.604	0.903	1.409
	10	0.389	0.681	0.999	1.446

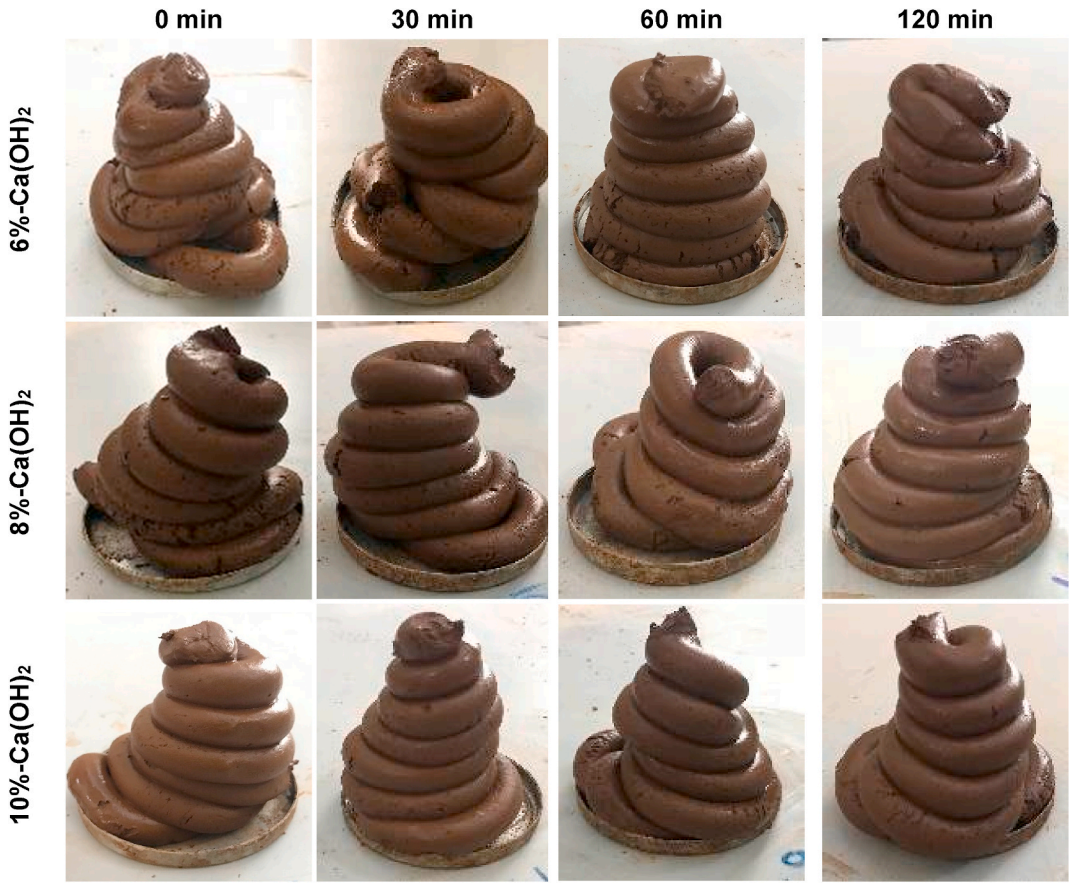

Fig. 16. Samples after ram extrusion.

these elements are not the focus of this research. 3D-AM application at laboratory scale was performed using a 3D printer to demonstrate the feasibility of printing CDW-based geopolymers developed in the current research. Fig. 17 shows the details of the 3D-printer used in the laboratory. After preliminary testing, the optimum printer speed was set at 16 mm/s, based on the flow rate of the pump and the circular nozzle used during the printing process. The geopolymer mixture activated by the binary use of 6.25M-NaOH and %10-$Ca(OH)_2$ was chosen for the laboratory-scale 3D-printing process.

For 3D-AM, bond strength, and thereby adhesion between the printed layers during fresh and hardened state should be significant; unless strength is developed between layers during these states, the structure can collapse in a small quake or even due to the dead load. Fig. 18 shows the visual inspections performed on the printed structure to offer an idea of the selected mixture's quality in forming bonds between the printed layers.

As seen from Fig. 18, for, no cracks/voids/defects were observed for both the internal and external structures, suggesting an adequate

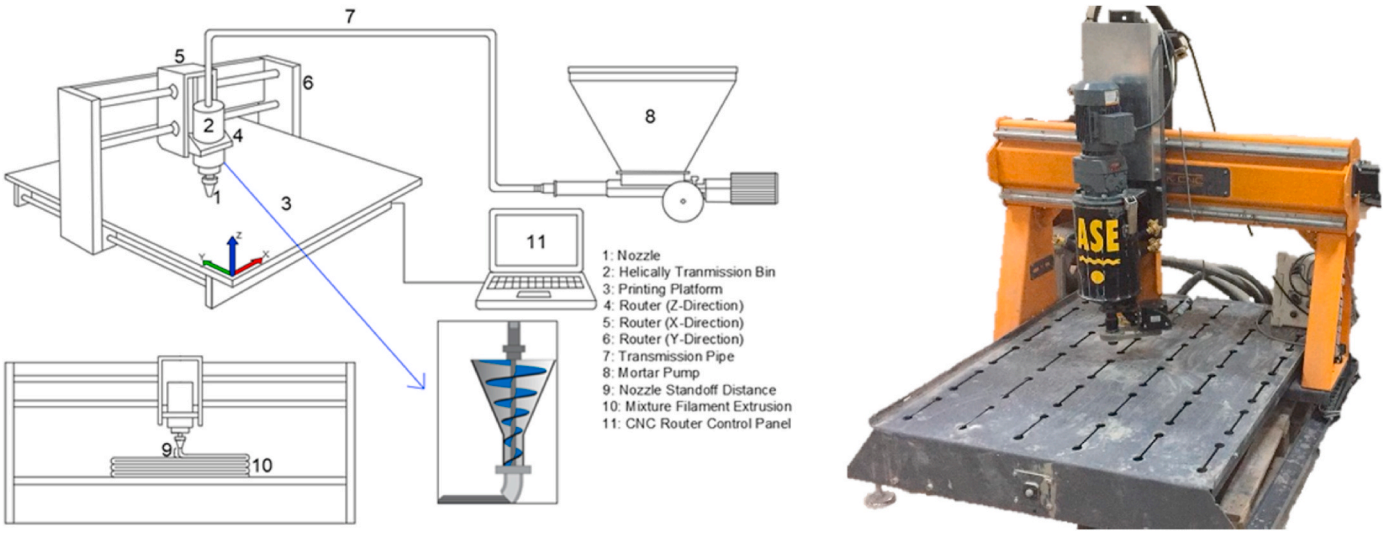

Fig. 17. Details of the 3D-printer used in the laboratory.

Fig. 18. Internal and external structure showing general bond behavior between printed layers.

adhesion between the layers. It should be noted that different in-depth test methods have been used in literature to evaluate the bond strength of the printed layers. However, the current research is a preliminary work aiming to show the possible printability of CDW-based geopolymers. Therefore, no detailed investigations regarding bond strength of printed layers have been included here, although this will be done in future work.

A designed structure was printed to investigate the real-time performance of the CDW-based geopolymers in regard to shape retention, buildability, extrudability and the relationship between designed and printed structure. Fig. 19 shows G-code provisions for the structure to be printed along with the product design, production process, and ultimate printed. As seen from the figure, the CDW-based geopolymer mixture without additional chemical admixtures performed satisfactorily in terms of buildability, shape retention, and extrudability, and had adequate open-time of nearly 1 h without considerable loss of flowability. This confirms the capability of the empirical test methods used to evaluate the fresh and hardened properties of the mixtures to determine their adequacy for 3D-AM applications.

4. Conclusions

The following conclusions have been drawn from the experimental works performed within the scope of the current research:

- Single use of NaOH as an alkaline activator had different impacts on the rheological properties of CDW-based geopolymers with varying molarities. Rheological behavior changed considerably for mixtures activated with 6.25M- and 11.25M-NaOH. When activated by 6.25M-NaOH, sudden increases were observed in flowability and decreases in vane shear stress and buildability. As molarity increased up to 11.25M-NaOH, flowability increased and buildability and vane shear stress decreased gradually. However, after 11.25 M, although buildability and vane shear stress continued to decrease, flowability began to decrease as well. These decrements in flowability were attributed to the sticky gel formation and inadequateness of the flow table test method to overcome the cohesiveness of mixtures. After 25M-NaOH, tests could not be performed as the mixtures stuck to the ring mold used for both buildability and flow table tests.
- Use of $Ca(OH)_2$ made the matrix more viscous, lowered flowability and increased buildability and vane shear stress in most cases. It had similar influence in both binary use with NaOH and ternary use with NaOH and Na_2SiO_3.
- Na_2SiO_3 dramatically decreased the viscosity of the mixtures and resulted in increments in flowability and decrements in buildability and vane shear stress. However, Na_2SiO_3 accelerated geopolymerization, hence shortening the setting/open-time period of mixtures, which was not suitable for 3D-AM.
- Single use of NaOH could not provide adequate compressive strength development, with a maximum of 10.8 MPa strength recorded after 28 days of ambient curing. Although $Ca(OH)_2$ increased the

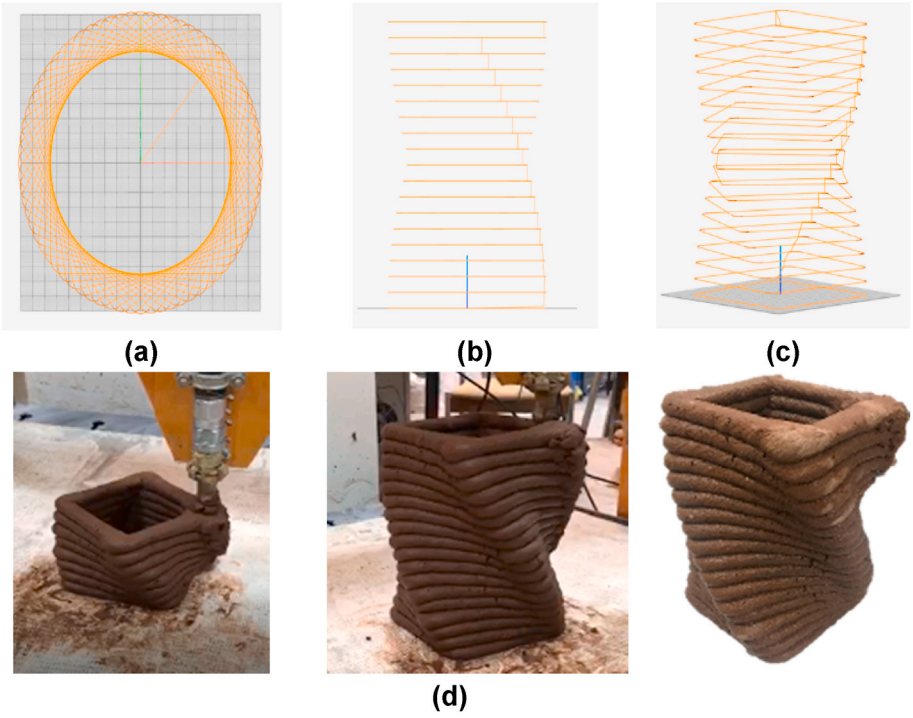

Fig. 19. Provision of the G-codes of the designed structure on software (a) top view (b) side view (c) 3D model and (d) different steps of 3D-printing structure.

compressive strength, after 10M-NaOH, compressive strength development was not observed for binary use of $Ca(OH)_2$ with NaOH. Na_2SiO_3 increased the compressive strength of mixtures in which a ternary combination of activators was used, although binary use of NaOH and Na_2SiO_3 did not contribute to increments in compressive strength.

- Mixtures activated with the binary use of 6.25M-NaOH and 6-10%-$Ca(OH)_2$ were used for ram extrusion as the rheological properties and compressive strength of these mixtures were found to be more suitable for 3D-AM purposes. Visual inspection of the extruded structure showed that the mixture with 6.25M-NaOH and 10%-Ca $(OH)_2$ had better printability given the formation of fewer defects, voids, and less discontinuity.
- Vane shear tests were insufficient compared to ram extrusion in showing the effect of $Ca(OH)_2$ addition on viscosity, as the sensitivity of the vane shear apparatus was much lower than that of the ram extruder. However, increments in shear stresses were observed in both testing methods during the open-time performance assessment.
- Product printed via laboratory-scale printer showed that entirely CDW-based geopolymers could be used for 3D-AM applications without any additional chemical admixtures, and that empirical test methods could be used to evaluate the suitability of these mixtures for applicability in 3D-AM.

Declaration of competing interest

The authors declare that they have no known competing financial interests or personal relationships that could have appeared to influence the work reported in this paper.

Acknowledgement

The authors gratefully acknowledge the financial assistance of the Scientific and Technical Research Council (TUBITAK) of Turkey provided under Project: 119M630 and 119N030. This publication is a part of doctoral dissertation work by the first author in the Academic Program of Civil Engineering, Institute of Science, Hacettepe University.

References

[1] B.B. Sabir, S. Wild, J. Bai, Metakaolin and calcined clays as pozzolans for concrete: a review, Cement Concr. Compos. 23 (2001) 441–454, https://doi.org/10.1016/S0958-9465(00)00092-5.
[2] P. Cachim, A. Velosa, E. Ferraz, Substitution materials for sustainable concrete production in Portugal, KSCE J. Civ. Eng. 18 (2013) 60–66, https://doi.org/10.1007/s12205-014-0201-3.
[3] D. Mckelvey, V. Sivakumar, A. Bell, G. Mclaverty, Shear strength of recycled construction materials intended for use in vibro ground improvement, Proc. Inst. Civ. Eng. - Gr. Improv. 6 (2002) 59–68, https://doi.org/10.1680/grim.2002.6.2.59.
[4] M.M.A.B. Abdullah, A. Abdullah, H. Mohammed, H. Kamarudin, K. Nizar, Z. Yahya, Review on fly ash-based geopolymer concrete without Portland Cement, J. Eng. Technol. Res. 3 (2011) 1–4.
[5] P. Duxson, A. Fernández-Jiménez, J.L. Provis, G.C. Lukey, A. Palomo, J.S.J. Van Deventer, Geopolymer technology: the current state of the art, J. Mater. Sci. 42 (2006) 2917–2933, https://doi.org/10.1007/s10853-006-0637-z.
[6] N. Hamdi, I. Ben Messaoud, E. Srasra, Production of geopolymer binders using clay minerals and industrial wastes, Compt. Rendus Chem. 22 (2019) 220–226, https://doi.org/10.1016/j.crci.2018.11.010.
[7] C. Shi, B. Qu, J.L. Provis, Recent progress in low-carbon binders, Cement Concr. Res. 122 (2019) 227–250, https://doi.org/10.1016/j.cemconres.2019.05.009.
[8] C.S. Poon, A.T.W. Yu, L.H. Ng, On-site sorting of construction and demolition waste in Hong Kong, Resour. Conserv. Recycl. 32 (2001) 157–172, https://doi.org/10.1016/S0921-3449(01)00052-0.
[9] H. Ulugöl, A. Kul, G. Yıldırım, M. Şahmaran, A. Aldemir, D. Figueira, A. Ashour, Mechanical and microstructural characterization of geopolymers from assorted construction and demolition waste-based masonry and glass, J. Clean. Prod. 280 (2021) 124358, https://doi.org/10.1016/j.jclepro.2020.124358.
[10] G. Yıldırım, A. Kul, E. Özçelikci, M. Şahmaran, A. Aldemir, D. Figueira, A. Ashour, Development of alkali-activated binders from recycled mixed masonry-originated waste, J. Build. Eng. 33 (2021) 101690, https://doi.org/10.1016/j.jobe.2020.101690.
[11] A. Allahverdi, E. Najafi Kani, Construction wastes as raw materials for geopolymer binders, Int. J. Civ. Eng. 7 (2009) 154–160.
[12] L. Reig, M.M. Tashima, L. Soriano, M. V Borrachero, J. Monzó, J. Payá, Alkaline activation of ceramic waste materials, Waste Biomass Valoriz. 4 (2013) 729–736, https://doi.org/10.1007/s12649-013-9197-z.
[13] K. Komnitsas, D. Zaharaki, A. Vlachou, G. Bartzas, M. Galetakis, Effect of synthesis parameters on the quality of construction and demolition wastes (CDW) geopolymers, Adv. Powder Technol. 26 (2015) 368–376, https://doi.org/10.1016/j.apt.2014.11.012.
[14] G. Silva, D. Castañeda, S. Kim, A. Castañeda, B. Bertolotti, L. Ortega-San-Martin, J. Nakamatsu, R. Aguilar, Analysis of the production conditions of geopolymer matrices from natural pozzolana and fired clay brick wastes, Construct. Build. Mater. 215 (2019) 633–643, https://doi.org/10.1016/j.conbuildmat.2019.04.247.
[15] R.A. Robayo-Salazar, J.F. Rivera, R. Mejía de Gutiérrez, Alkali-activated building materials made with recycled construction and demolition wastes, Construct. Build. Mater. 149 (2017) 130–138, https://doi.org/10.1016/j.conbuildmat.2017.05.122.
[16] R. Xiao, Y. Ma, X. Jiang, M. Zhang, Y. Zhang, Y. Wang, B. Huang, Q. He, Strength, microstructure, efflorescence behavior and environmental impacts of waste glass geopolymers cured at ambient temperature, J. Clean. Prod. 252 (2020) 119610, https://doi.org/10.1016/j.jclepro.2019.119610.
[17] M. Torres-Carrasco, F. Puertas, Waste glass in the geopolymer preparation. Mechanical and microstructural characterisation, J. Clean. Prod. 90 (2015) 397–408, https://doi.org/10.1016/j.jclepro.2014.11.074.
[18] M. Cyr, R. Idir, T. Poinot, Properties of inorganic polymer (geopolymer) mortars made of glass cullet, J. Mater. Sci. 47 (2012) 2782–2797, https://doi.org/10.1007/s10853-011-6107-2.
[19] M. Vafaei, A. Allahverdi, High strength geopolymer binder based on waste-glass powder, Adv. Powder Technol. 28 (2017) 215–222, https://doi.org/10.1016/j.apt.2016.09.034.
[20] S. Dadsetan, H. Siad, M. Lachemi, M. Sahmaran, Construction and demolition waste in geopolymer concrete technology: a review, Mag. Concr. Res. 71 (2019) 1232–1252, https://doi.org/10.1680/jmacr.18.00307.
[21] E. Lloret, A.R. Shahab, M. Linus, R.J. Flatt, F. Gramazio, M. Kohler, S. Langenberg, Complex concrete structures: merging existing casting techniques with digital fabrication, Comput. Des. 60 (2015) 40–49, https://doi.org/10.1016/j.cad.2014.02.011.
[22] A. Perrot, D. Rangeard, A. Pierre, Structural built-up of cement-based materials used for 3D-printing extrusion techniques, Mater. Struct. Constr. 49 (2015) 1213–1220, https://doi.org/10.1617/s11527-015-0571-0.
[23] G. Cesaretti, E. Dini, X. De Kestelier, V. Colla, L. Pambaguian, Building components for an outpost on the Lunar soil by means of a novel 3D printing technology, Acta Astronaut. 93 (2014) 430–450, https://doi.org/10.1016/j.actaastro.2013.07.034.
[24] B. Panda, S.C. Paul, N.A.N. Mohamed, Y.W.D. Tay, M.J. Tan, Measurement of tensile bond strength of 3D printed geopolymer mortar, Measurement 113 (2018) 108–116, https://doi.org/10.1016/j.measurement.2017.08.051.
[25] J.H. Lim, B. Panda, Q.-C. Pham, Improving flexural characteristics of 3D printed geopolymer composites with in-process steel cable reinforcement, Construct. Build. Mater. 178 (2018) 32–41, https://doi.org/10.1016/j.conbuildmat.2018.05.010.
[26] B. Panda, M.J. Tan, Experimental study on mix proportion and fresh properties of fly ash based geopolymer for 3D concrete printing, Ceram. Int. 44 (2018) 10258–10265, https://doi.org/10.1016/j.ceramint.2018.03.031.
[27] M. Xia, J. Sanjayan, Method of formulating geopolymer for 3D printing for construction applications, Mater. Des. 110 (2016) 382–390, https://doi.org/10.1016/j.matdes.2016.07.136.
[28] M. Xia, J.G. Sanjayan, Methods of enhancing strength of geopolymer produced from powder-based 3D printing process, Mater. Lett. 227 (2018) 281–283, https://doi.org/10.1016/j.matlet.2018.05.100.
[29] B. Panda, C. Unluer, M.J. Tan, Investigation of the rheology and strength of geopolymer mixtures for extrusion-based 3D printing, Cement Concr. Compos. 94 (2018) 307–314, https://doi.org/10.1016/j.cemconcomp.2018.10.002.
[30] B. Panda, N.A.N. Mohamed, S.C. Paul, G.V.P.B. Singh, M.J. Tan, B. Šavija, The effect of material fresh properties and process parameters on buildability and interlayer adhesion of 3D printed concrete, Materials 12 (2019), https://doi.org/10.3390/ma12132149.
[31] G. Ma, Z. Li, L. Wang, G. Bai, Micro-cable reinforced geopolymer composite for extrusion-based 3D printing, Mater. Lett. 235 (2019) 144–147, https://doi.org/10.1016/j.matlet.2018.09.159.
[32] T. Tho-In, V. Sata, K. Boonserm, P. Chindaprasirt, Compressive strength and microstructure analysis of geopolymer paste using waste glass powder and fly ash, J. Clean. Prod. 172 (2018) 2892–2898, https://doi.org/10.1016/j.jclepro.2017.11.125.
[33] J. Temuujin, A. van Riessen, R. Williams, Influence of calcium compounds on the mechanical properties of fly ash geopolymer pastes, J. Hazard Mater. 167 (2009) 82–88, https://doi.org/10.1016/j.jhazmat.2008.12.121.
[34] B. Panda, N.A. Noor Mohamed, M.J. Tan, Rheology and Structural Rebuilding of One-Part Geopolymer Mortar in the Context of 3D Concrete Printing, 2019, https://doi.org/10.1007/978-3-030-22566-7.
[35] J. Kruger, S. Zeranka, G. van Zijl, Quantifying Constructability Performance of 3D Concrete Printing via Rheology-Based Analytical Models, 2019.
[36] A. Kazemian, X. Yuan, E. Cochran, B. Khoshnevis, Cementitious materials for construction-scale 3D printing: laboratory testing of fresh printing mixture, Construct. Build. Mater. 145 (2017) 639–647, https://doi.org/10.1016/j.conbuildmat.2017.04.015.
[37] Y. Kim, H.-J. Kong, V. Li, Design of engineered cementitious composite (ECC) suitable for wet-mix shotcreting, ACI Mater. J. 100 (2003).
[38] K. Khayat, A. Omran, S. Naji, P. Billberg, A. Yahia, Test Methods to Evaluate Form Pressure of SCC, 2008, pp. 308–314.

[39] M.A. Abd Elaty, M.F. Ghazy, Flow properties of fresh concrete by using modified geotechnical Vane shear test, HBRC J. 8 (2012) 159–169, https://doi.org/10.1016/j.hbrcj.2012.07.001.

[40] G. Tabilo-Munizaga, G. V Barbosa-Cánovas, Rheology for the food industry, J. Food Eng. 67 (2005) 147–156, https://doi.org/10.1016/j.jfoodeng.2004.05.062.

[41] R. Alfani, G.L. Guerrini, Rheological test methods for the characterization of extrudable cement-based materials - a review, Mater. Struct. Constr. 38 (2005) 239–247, https://doi.org/10.1617/14191.

[42] X. Zhou, Z. Li, Characterization of rheology of fresh fiber reinforced cementitious composites through ram extrusion, Mater. Struct. 38 (2005) 17–24, https://doi.org/10.1007/BF02480570.

[43] K. Kuder, S. Shah, Rheology of extruded cement-based materials, ACI Mater. J., 2007, pp. 479–484, https://doi.org/10.1007/978-1-4020-5104-3_58.

[44] A. Perrot, Y. Mélinge, D. Rangeard, F. Micaelli, P. Estellé, C. Lanos, Use of ram extruder as a combined rheo-tribometer to study the behaviour of high yield stress fluids at low strain rate, Rheol. Acta 51 (2012) 743–754, https://doi.org/10.1007/s00397-012-0638-6.

[45] Y. Chen, S. Chaves Figueiredo, Ç. Yalçınkaya, O. Çopuroğlu, F. Veer, E. Schlangen, The effect of viscosity-modifying admixture on the extrudability of limestone and calcined clay-based cementitious material for extrusion-based 3D concrete printing, Materials 12 (2019) 1374, https://doi.org/10.3390/ma12091374.

[46] H. Ogura, V.N. Nerella, V. Mechtcherine, Developing and testing of strain-hardening cement-based composites (SHCC) in the context of 3D-printing, Materials 11 (2018) 1375, https://doi.org/10.3390/ma11081375.

[47] V.N. Nerella, M. Näther, A. Iqbal, M. Butler, V. Mechtcherine, Inline quantification of extrudability of cementitious materials for digital construction, Cement Concr. Compos. 95 (2019) 260–270, https://doi.org/10.1016/j.cemconcomp.2018.09.015.

[48] S. Chaves Figueiredo, C. Romero Rodríguez, Z.Y. Ahmed, D.H. Bos, Y. Xu, T. M. Salet, O. Çopuroğlu, E. Schlangen, F.P. Bos, An approach to develop printable strain hardening cementitious composites, Mater. Des. 169 (2019) 107651, https://doi.org/10.1016/j.matdes.2019.107651.

[49] J.J. Benbow, E.W. Oxley, J. Bridgwater, The extrusion mechanics of pastes—the influence of paste formulation on extrusion parameters, Chem. Eng. Sci. 42 (1987) 2151–2162, https://doi.org/10.1016/0009-2509(87)85036-4.

[50] R.A. Basterfield, C.J. Lawrence, M.J. Adams, On the interpretation of orifice extrusion data for viscoplastic materials, Chem. Eng. Sci. 60 (2005) 2599–2607, https://doi.org/10.1016/j.ces.2004.12.019.

[51] X. Zhou, Z. Li, M. Fan, H. Chen, Rheology of semi-solid fresh cement pastes and mortars in orifice extrusion, Cement Concr. Compos. 37 (2013) 304–311, https://doi.org/10.1016/j.cemconcomp.2013.01.004.

[52] A. Perrot, D. Rangeard, V.N. Nerella, V. Mechtcherine, Extrusion of cement-based materials - an overview, RILEM Tech. Lett. 3 (2019), https://doi.org/10.21809/rilemtechlett.2018.75.

[53] R.V. Mises, Mechanik der festen Körper im plastisch-deformablen Zustand. [Mechanics of Solid Bodies in Plastic Deformation State, Nachrichten von Der Gesellschaft Der Wissenschaften Zu Gottingen (Mathematisch-Physikalische Klasse) 1 (1913) 582–592.

[54] J.J. Benbow, J. Bridgwater, The influence of formulation on extrudate structure and strength, Chem. Eng. Sci. 42 (1987) 753–766, https://doi.org/10.1016/0009-2509(87)80035-0.

[55] B. Nematollahi, P. Vijay, J. Sanjayan, A. Nazari, M. Xia, V.N. Nerella, V. Mechtcherine, Effect of polypropylene fibre addition on properties of geopolymers made by 3D printing for digital construction, Materials 11 (2018) 2352, https://doi.org/10.3390/ma11122352.

[56] H. Xu, J.S.J. Van Deventer, The geopolymerisation of alumino-silicate minerals, Int. J. Miner. Process. 59 (2000) 247–266, https://doi.org/10.1016/S0301-7516(99)00074-5.

[57] A. Palomo, S. Alonso, A. Fernández-Jiménez, I. Sobrados, J. Sanz, Alkaline activation of fly ashes: NMR study of the reaction products, J. Am. Ceram. Soc. 87 (2008) 1141–1145, https://doi.org/10.1111/j.1551-2916.2004.01141.x.

[58] Y. Rifaai, A. Yahia, A. Mostafa, S. Aggoun, E.-H. Kadri, Rheology of fly ash-based geopolymer: effect of NaOH concentration, Construct. Build. Mater. 223 (2019) 583–594, https://doi.org/10.1016/j.conbuildmat.2019.07.028.

[59] H.A. Gasteiger, W.J. Frederick, R.C. Streisel, Solubility of aluminosilicates in alkaline solutions and a thermodynamic equilibrium model, Ind. Eng. Chem. Res. 31 (1992) 1183–1190, https://doi.org/10.1021/ie00004a031.

[60] D. Khale, R. Chaudhary, Mechanism of geopolymerization and factors influencing its development: a review, J. Mater. Sci. 42 (2007) 729–746, https://doi.org/10.1007/s10853-006-0401-4.

[61] S. Patankar, Y. Ghugal, S. Jamkar, Effect of concentration of sodium hydroxide and degree of heat curing on fly ash-based geopolymer mortar, Indian J. Mater. Sci. (2014), https://doi.org/10.1155/2014/938789, 2014.

[62] A. Malkawi, M. Nuruddin, A. Fauzi, H. Al-Mattarneh, B. Mohammed, Effects of alkaline solution on properties of the HCFA geopolymer mortars, Procedia Eng. 148 (2016) 710–717, https://doi.org/10.1016/j.proeng.2016.06.581.

[63] G.F. Huseien, M. Ismail, N.H.A. Khalid, M.W. Hussin, J. Mirza, Compressive strength and microstructure of assorted wastes incorporated geopolymer mortars: effect of solution molarity, Alexandria Eng. J. 57 (2018) 3375–3386, https://doi.org/10.1016/j.aej.2018.07.011.

[64] S. Alonso, A. Palomo, Alkaline activation of metakaolin and calcium hydroxide mixtures: influence of temperature, activator concentration and solids ratio, Mater. Lett. 47 (2001) 55–62, https://doi.org/10.1016/S0167-577X(00)00212-3.

[65] Y.-M. Liew, C.-Y. Heah, A.B. Mohd Mustafa, H. Kamarudin, Structure and properties of clay-based geopolymer cements: a review, Prog. Mater. Sci. 83 (2016) 595–629, https://doi.org/10.1016/j.pmatsci.2016.08.002.

[66] J. Feng, R. Zhang, L. Gong, Y. Li, W. Cao, X. Cheng, Development of porous fly ash-based geopolymer with low thermal conductivity, Mater. Des. 65 (2015) 529–533, https://doi.org/10.1016/j.matdes.2014.09.024.

[67] M. Granizo, S. Alonso, M. Blanco-Varela, A. Palomo, Alkaline activation of metakaolin: effect of calcium hydroxide in the products of reaction, J. Am. Ceram. Soc. 85 (2004) 225–231, https://doi.org/10.1111/j.1151-2916.2002.tb00070.x.

[68] X. Guo, H. Shi, L. Chen, W.A. Dick, Alkali-activated complex binders from class C fly ash and Ca-containing admixtures, J. Hazard Mater. 173 (2010) 480–486, https://doi.org/10.1016/j.jhazmat.2009.08.110.

[69] C.K. Yip, G.C. Lukey, J.S.J. van Deventer, The coexistence of geopolymeric gel and calcium silicate hydrate at the early stage of alkaline activation, Cement Concr. Res. 35 (2005) 1688–1697, https://doi.org/10.1016/j.cemconres.2004.10.042.

[70] C. Yip, J. Van Deventer, Microanalysis of calcium silicate hydrate gel formed within a geopolymeric binder, J. Mater. Sci. 38 (2003) 3851–3860, https://doi.org/10.1023/A:1025904905176.

[71] D. Hardjito, C. Cheak, C. Ho, Strength and setting times of low calcium fly ash-based geopolymer mortar, Mod. Appl. Sci. 2 (2008), https://doi.org/10.5539/mas.v2n4p3.

[72] O. Wattimena, A. Antoni, D. Hardjito, A review on the effect of fly ash characteristics and their variations on the synthesis of fly ash based geopolymer, in: AIP Conf. Proc., 2017, p. 20041, https://doi.org/10.1063/1.5003524.

[73] J. Zhang, S. Li, Z. Li, Q. Zhang, H. Li, J. Du, Y. Qi, Properties of fresh and hardened geopolymer-based grouts, Ceram. - Silikaty. 63 (2019) 164–173, https://doi.org/10.13168/cs.2019.0008.

[74] Y. Fan, S. Yin, Z. Wen, J. Zhong, Activation of fly ash and its effects on cement properties, Cement Concr. Res. 29 (1999) 467–472, https://doi.org/10.1016/S0008-8846(98)00178-1.

[75] J. Provis, J. Deventer, Alkali Activated Materials: State-Of-The-Art Report, RILEM TC 224-AAM, 2013, https://doi.org/10.1007/978-94-007-7672-2.

[76] K. Dombrowski-Daube, A. Buchwald, M. Weil, The influence of calcium content on the structure and thermal performance of fly ash based geopolymers, J. Mater. Sci. 42 (2007) 3033–3043, https://doi.org/10.1007/s10853-006-0532-7.

[77] A. Favier, J.-B. d'Espinose de Lacaillerie, N. Roussel, J. Hot, G. Habert, Flow properties of MK-based geopolymer pastes. A comparative study with standard Portland cement pastes, Soft Matter 10 (2013), https://doi.org/10.1039/c3sm51889b.

[78] X. Chen, A. Sutrisno, L. Struble, Effects of calcium on setting mechanism of metakaolin-based geopolymer, J. Am. Ceram. Soc. 101 (2017), https://doi.org/10.1111/jace.15249.

[79] P. Chindaprasirt, T. Chareerat, V. Sirivivatnanon, Workability and strength of coarse high calcium fly ash geopolymer, Cement Concr. Compos. 29 (2007) 224–229, https://doi.org/10.1016/j.cemconcomp.2006.11.002.

[80] A. Sathonsaowaphak, P. Chindaprasirt, K. Pimraksa, Workability and strength of lignite bottom ash geopolymer mortar, J. Hazard Mater. 168 (2009) 44–50, https://doi.org/10.1016/j.jhazmat.2009.01.120.

[81] C. Li, H. Sun, L. Li, A review: the comparison between alkali-activated slag (Si + Ca) and metakaolin (Si + Al) cements, Cement Concr. Res. 40 (2010) 1341–1349, https://doi.org/10.1016/j.cemconres.2010.03.020.

[82] A.R. Kotwal, Y.J. Kim, J. Hu, V. Sriraman, Characterization and early age physical properties of ambient cured geopolymer mortar based on class C fly ash, Int. J. Concr. Struct. Mater. 9 (2014) 35–43, https://doi.org/10.1007/s40069-014-0085-0.

[83] S. Goberis, V. Antonovich, Influence of sodium silicate amount on the setting time and EXO temperature of a complex binder consisting of high-aluminate cement, liquid glass and metallurgical slag, Cement Concr. Res. 34 (2004) 1939–1941, https://doi.org/10.1016/J.CEMCONRES.2004.01.004.

[84] T.-R. Yang, T.-P. Chang, B. Chen, J.-Y. Shih, W.-L. Lin, Effect of alkaline solutions on engineering properties of alkali-activated GGBFS paste, J. Mar. Sci. Technol. 20 (2012).

[85] M.B. Karakoç, İ. Türkmen, M.M. Maraş, F. Kantarci, R. Demirboğa, M. Uğur Toprak, Mechanical properties and setting time of ferrochrome slag based geopolymer paste and mortar, Construct. Build. Mater. 72 (2014) 283–292, https://doi.org/10.1016/j.conbuildmat.2014.09.021.

[86] A. Pallagi, A. Tasi, A. Gácsi, M. Csáti, I. Palinko, G. Peintler, P. Sipos, The solubility of Ca(OH)2 in extremely concentrated NaOH solutions at 25°C, Cent. Eur. J. Chem. 10 (2012), https://doi.org/10.2478/s11532-011-0145-0.

[87] X. Ouyang, Y. Ma, Z. Liu, J. Liang, G. Ye, Effect of the sodium silicate modulus and slag content on fresh and hardened properties of alkali-activated fly ash/slag, Minerals 10 (2019) 15, https://doi.org/10.3390/min10010015.

[88] J.L. Provis, S.L. Yong, P. Duxson, 5 - nanostructure/microstructure of metakaolin geopolymers, in: J.L. Provis, J.S.J. van Deventer (Eds.), Geopolymers, Woodhead Publishing, 2009, pp. 72–88, https://doi.org/10.1533/9781845696382.1.72.

[89] G. De Schutter, K. Lesage, V. Mechtcherine, V.N. Nerella, G. Habert, I. Agusti-Juan, Vision of 3D printing with concrete — Technical, economic and environmental potentials, Cement Concr. Res. 112 (2018) 25–36, https://doi.org/10.1016/j.cemconres.2018.06.001.